

## USE AUTHORIZATION

In presenting this thesis in partial fulfillment of the requirements for an advanced degree at Idaho State University, I agree that the Library shall make it freely available for inspection. I further state that permission to download and/or print my thesis for scholarly purposes may be granted by the Dean of the Graduate School, Dean of my academic division, or by the University Librarian. It is understood that any copying or publication of this thesis for financial gain shall not be allowed without my written permission.

Signature \_\_\_\_\_

Date \_\_\_\_\_

CHARACTERIZATION OF THE NOVEL BACTERIAL  
ADENYLYL CYCLASE EFFECTOR, EXOY

by

Michael V. Madrid

A thesis

submitted in partial fulfillment

of the requirements for the degree of

Master of Science in Microbiology from

the Department of Biological Sciences

Idaho State University, Pocatello, Idaho

Spring 2014

Copyright (2014) Michael V. Madrid

## COMMITTEE APPROVAL

To the Graduate Faculty:

The members of the committee appointed to examine the thesis of Michael V. Madrid find it satisfactory and recommend that it be accepted.

---

Marc A. Benson, Ph.D.  
Major Advisor

---

Caryn Evilia, Ph.D.  
Committee Member

---

Rachel Smetanka, Ph.D., PA-C  
Graduate Faculty Representative

## TABLE OF CONTENTS

	<u>Page</u>
List of Figures	vi
List of Tables	viii
Abstract	ix
Hypothesis and Specific Aims	x
Chapter I: Introduction	1
Chapter II: Methods	15
Chapter III: Results	25
Chapter IV: Discussion	52
References	57

## LIST OF FIGURES

		<u>Page</u>
Figure 1	Bacterial Secretion Systems	7
Figure 2	ExsA Regulatory Cascade	10
Figure 3	Polymerase Chain Reaction <i>exoY</i> Gene Product	26
Figure 4	Representative Ligation Products	27
Figure 5	Translation of <i>exoY</i> Sequence	28
Figure 6	Translation of pET28 <i>exoYK81M</i> Sequence	29
Figure 7	Induction of Recombinant ExoY	30
Figure 8	Recombinant ExoY (K81M) Purification Scheme	32
Figure 9	Densitometric Quantification of rExoY (K81M)	33
Figure 10	Protein Profile of the Chromatography Steps Used to Prepare rExoY for Antibody Production	34
Figure 11	Validation of the cAMP EIA Standard Curve.	36
Figure 12	Effect of Dithiothreitol (DTT) on the cAMP EIA	37
Figure 13	Accuracy of the ExoY Activity Assay/cAMP EIA	38
Figure 14	Pull Down using rExoY as Bait and A549 Soluble Lysate as Prey Yielded Three Activator Candidates	40
Figure 15	Size Exclusion Chromatography A549 Protein Profile and rExoY Activity	41
Figure 16	Protein Profile of A549 Lysate Separated by Anion Exchange	42

Figure 17	rExoY-Mediated cAMP Production is Highest in the A549 High Density Lipid	43
Figure 18	Effect of Sodium Dodecyl Sulfate (SDS) on Proteinase K Activity	45
Figure 19	Optimal Concentration of Proteinase K for the A549 Digestion Reaction	46
Figure 20	Effects of the Protease Inhibitor Cocktail on Proteinase K	47
Figure 21	Effect of Protease Inhibitors on Proteinase K	49
Figure 22	Effect of Proteinase K and Inhibitor PMSF on rExoY	50
Figure 23	rExoY Activity after A549 Proteolysis	51

## LIST OF TABLES

		<u>Page</u>
Table 1	Primer Characteristics	16
Table 2	Strains and Vectors	18

**CHARACTERIZATION OF THE NOVEL BACTERIAL  
ADENYLYL CYCLASE EFFECTOR, EXOY**

**Thesis Abstract – Idaho State University – 2014**

*Pseudomonas aeruginosa* is an opportunistic pathogen that causes respiratory tract infections in immunocompromised patients. *P. aeruginosa* utilizes a Type 3 Secretion System (T3SS) to secrete up to four effectors (ExoS, ExoT, ExoU, and ExoY) directly into the eukaryotic cytosol during infection. ExoY is a class II bacterial adenylyl cyclase, but unlike the major members of this group, ExoY is activated by a calmodulin-independent mechanism. The activity of rExoY in the presence of the A549 lung epithelial cell lysate was assessed using an enzyme immunoassay (EIA) to detect the product of ExoY, cAMP. The sediment after A549 lysate ultracentrifugation activated rExoY five times more than the soluble lysate. To determine if rExoY was activated by a proteinaceous factor, we optimized a digestion of the soluble lysate using Proteinase K and observed that the activity of the fraction decreased substantially after proteolysis, indicating that the activator is proteinaceous.

## **HYPOTHESIS AND SPECIFIC AIMS**

My hypothesis was that ExoY is a novel bacterial adenylyl cyclase effector that is activated by a non-calmodulin eukaryotic factor. To test my hypothesis, I proposed three aims: the first was the cloning, expression, and purification of ExoY and the catalytic null K81M, followed by the optimization of the ExoY activity assay and cAMP EIA, and finally, the enrichment of the ExoY activator.

## CHAPTER I: INTRODUCTION

### General Characteristics

*Pseudomonas aeruginosa* (*P. aeruginosa*) is a Gram-negative facultative anaerobe and serves as the type species of the genus *Pseudomonas* [1, 2]. *P. aeruginosa* is historically known for its secretion of pyocyanin, a blue-green pigment [3] that causes the colony to turn blue-green. Indeed, pyocyanin is the origin of the species name *aeruginosa*, which comes from the Latin *aeruginosus*, meaning covered in verdigris, or copper rust [4]. Isolated colonies of *P. aeruginosa* appear as large, flat, greenish colonies with irregular margins and a metallic luster, and have a distinctive fragrance reminiscent of an artificial grape scent or tortillas. The size of an individual cell ranges from approximately 0.5 – 0.8 by 1.5 – 3.0  $\mu\text{m}$  [5]. *P. aeruginosa* is monotrichous and is catalase and oxidase positive; the oxidase test is used to differentiate *P. aeruginosa* from *Enterobacteriaceae*. It is a non-fermenter of carbohydrates and is methyl red and Voges-Proskauer negative, indole negative, and citrate positive [2].

The ~6.3 Mbp genome of *P. aeruginosa* is large compared to the genomes of other common bacteria, such as *Staphylococcus aureus* (~2.8 Mbp) and *Escherichia coli* (~5 Mbp), and encodes 5,572 open reading frames (ORFs) – nearly as many as the eukaryote *Saccharomyces cerevisiae* (6,349 ORFs) [6]. Because of its large genome, *P. aeruginosa* is capable of living in a variety of environments. Such environments include a wide range of temperatures [2], colonization of patient endotracheal tubes [7, 8], and even harsh environments such as sites polluted by crude oil, where *P. aeruginosa* has been shown to degrade hydrocarbons in tarballs [9, 10]. Additionally, *P. aeruginosa* is capable of adapting to microgravity, as cultures on the Mir International Space Station

have demonstrated a new column-and-canopy biofilm architecture [11]. The ubiquity of *P. aeruginosa*, in addition to its numerous virulence factors and ability to infect many different organisms, make it a vital target for further study.

## **Clinical Significance**

### **General Infections**

Despite its role as an opportunistic pathogen, *P. aeruginosa* can also cause acute infections in patients who are not considered immunocompromised. If *P. aeruginosa* is introduced to the eye through trauma or contact lens contamination, it can cause keratitis, or a scleral abscess [12]. Immediate treatment is necessary to prevent the host's inflammatory response from causing corneal scarring, which can lead to blindness [13]. More frequently, however, *P. aeruginosa* causes dermatitis, or "hot tub rash," as a result of exposure to inadequately maintained hot tub water. Symptoms include itchy spots that become bumpy red rashes, particularly in areas covered by a swimsuit, and can progress to pus-filled blisters around the hair follicles [12, 14].

### **Ventilator-Associated Pneumonia**

*P. aeruginosa* commonly causes nosocomial infections, colonizing the endotracheal tube of patients undergoing mechanical ventilation and resulting in ventilator-associated pneumonia (VAP) [15]. Specifically, VAP refers to a pneumonia that occurs more than 48 hours after patients have received mechanical ventilation. VAP that occurs within the first 4 days of hospitalization is referred to as early-onset and carries a good prognosis. After 4 days, it is considered late-onset VAP; which is more

likely to be caused by multi-drug resistance and an increase in patient mortality [16]. Between 250,000 and 300,000 cases occur in the United States per year, or approximately 5 to 10 cases per 1,000 hospital admissions [8]. Of these cases, *P. aeruginosa* is one of the most common Gram-negative isolates from patients with VAP, along with *Acinetobacter baumannii* [17, 18]. In a 2013 study conducted by Golia, et al., 40% of *P. aeruginosa* isolates in an Indian tertiary care intensive care unit were resistant to all groups of antibiotics. The reported mortality of VAP has been as high as 50%, in part due to the natural antimicrobial resistance in many strains of *P. aeruginosa*, which can significantly worsen the prognosis of VAP [8]. *P. aeruginosa*-associated VAP is a vital issue in healthcare settings worldwide, particularly in underdeveloped countries.

## **Burns**

As an opportunistic pathogen, *P. aeruginosa* targets damaged tissue such as burn wounds. An open burn wound promotes the growth of a variety of microorganisms due to the healing-induced inhibition of the immune response [19]. Generally, the burn wound is first colonized by endogenous microorganisms from the victim's normal skin, respiratory, and gastrointestinal flora, followed by exogenous fungal organisms after broad-spectrum antibiotic therapy reduces the bacterial population [7]. *P. aeruginosa* contaminates the burn wound from the environment or from exposure to contaminated health care workers. Unfortunately, many strains of *P. aeruginosa* that have been isolated in health care settings are frequently resistant to a wide variety of antibiotics [16, 17, 20]. This antibiotic resistance provides the opportunity for *P. aeruginosa* to establish an infection, which only increases the mortality rate [7].

## **Cystic Fibrosis**

Cystic fibrosis (CF) is a lethal autosomal recessive genetic disorder caused by mutations in the gene for the CF transmembrane conductance regulator (CFTR) chloride channel, which regulates the movement of sodium and chloride anions across epithelial membranes [21, 22]. A lack of ion movement causes water to move from the normally isosmotic airway surface liquid into the cell, increasing the mucus concentration, which sticks to the epithelial surface and flattens the cilia [22]. This increased amount of mucus creates microaerobic, or anaerobic conditions, which has been shown to upregulate alginate production; this can limit oxygen diffusion into the alveoli, further aggravating hypoxia [23, 24]. Young patients with CF often develop *P. aeruginosa* infections and by adulthood 80% of all CF patients have chronic *P. aeruginosa* infections [22, 25].

## **Antibiotic Resistance**

*P. aeruginosa* has a natural resistance to a wide variety of antibiotics, which is owed to a number of factors, including  $\beta$ -lactamase proteins, multidrug efflux pumps, acquisition of antibiotic resistance genes, and natural mutations. *P. aeruginosa* expresses endogenous  $\beta$ -lactamases and has acquired exogenous  $\beta$ -lactamase genes through horizontal gene transfer [26].  $\beta$ -lactamases are capable of hydrolyzing  $\beta$ -lactam antibiotics like the penicillins, monobactams, and cephalosporins [26]. A selected mutation in the *oprD* gene results in a loss of the outer membrane porin protein OprD. Without OprD, carbapenem antibiotics such as imipenem and meropenem are prevented from entering the cell and inhibiting cell wall synthesis during binary fission [27, 28].

Multidrug efflux pumps in the cytoplasmic membrane are able to remove a variety of antibiotics from the cell [29].

## **Virulence Factors**

### **Exotoxin A**

Exotoxin A (ETA) is a 66 kDa extracellular protein that is comprised of three domains: receptor-binding, translocation, and catalytic [30, 31]. ETA is secreted by the *P. aeruginosa* type II secretion system (T2SS) [32]. After transportation into the periplasm across the inner membrane, ETA is transported directly into the environment through a pore composed of a complex of secretin proteins that make up the T2SS [33]. ETA enters the eukaryotic host cell via receptor-mediated endocytosis, and is translocated across the endosomal membrane into the cytosol upon the acidification of the endosome [34]. Once in the cytosol, ETA causes cell death due to the ADP-ribosylation of eukaryotic elongation factor 2 (eEF2), a protein that is essential to eukaryotic translation [30]. One of *P. aeruginosa*'s most effective virulence factors, ETA has an LD<sub>50</sub> of 0.2 µg/animal on intraperitoneal injection into mice [35].

### **Elastase**

The elastase produced by *P. aeruginosa* was first described in 1965 [36]. Elastase has non-specific proteolytic activity which improves *P. aeruginosa* motility through the host tissue by digesting tight junction proteins [36–38]. The proteolytic properties are capable of digesting lysozyme to prevent bacteriolysis [39], pulmonary surfactant

protein-A to prevent phagocytosis, and antibacterial peptides, cytokines, chemokines, and immunoglobulins to inhibit the host's immune response [40].

### **Pyocyanin**

Pyocyanin is a blue-green pigment produced by *P. aeruginosa* which has been shown to interfere with ciliary beating [41], induce apoptosis in neutrophils [42], and effect secretion of Ig by B-lymphocytes [43]. A redox-active compound, pyocyanin also has antimicrobial properties due to its ability to initiate a redox cascade via NADH or NADPH [44].

### **Alginate**

Alginate is an exopolysaccharide secreted by mucoid strains of *P. aeruginosa* [45]. Alginate production is regulated by *algD*, which is transcriptionally activated in the presence of high concentrations of electrolytes and under anaerobic conditions [23, 46, 47]. As a viscous secretion, alginate is responsible for the production of biofilms and can prevent phagocytosis of the bacterial cell during the immune response [48, 49]. Alginate can decrease oxygen diffusion in patients with cystic fibrosis, which can further aggravate hypoxia [23].

### **Bacterial Secretion Systems**

There are several types of secretion systems used by Gram-negative bacteria. The Type I Secretion System (T1SS) (Figure 1A) consists of three proteins that span the cell

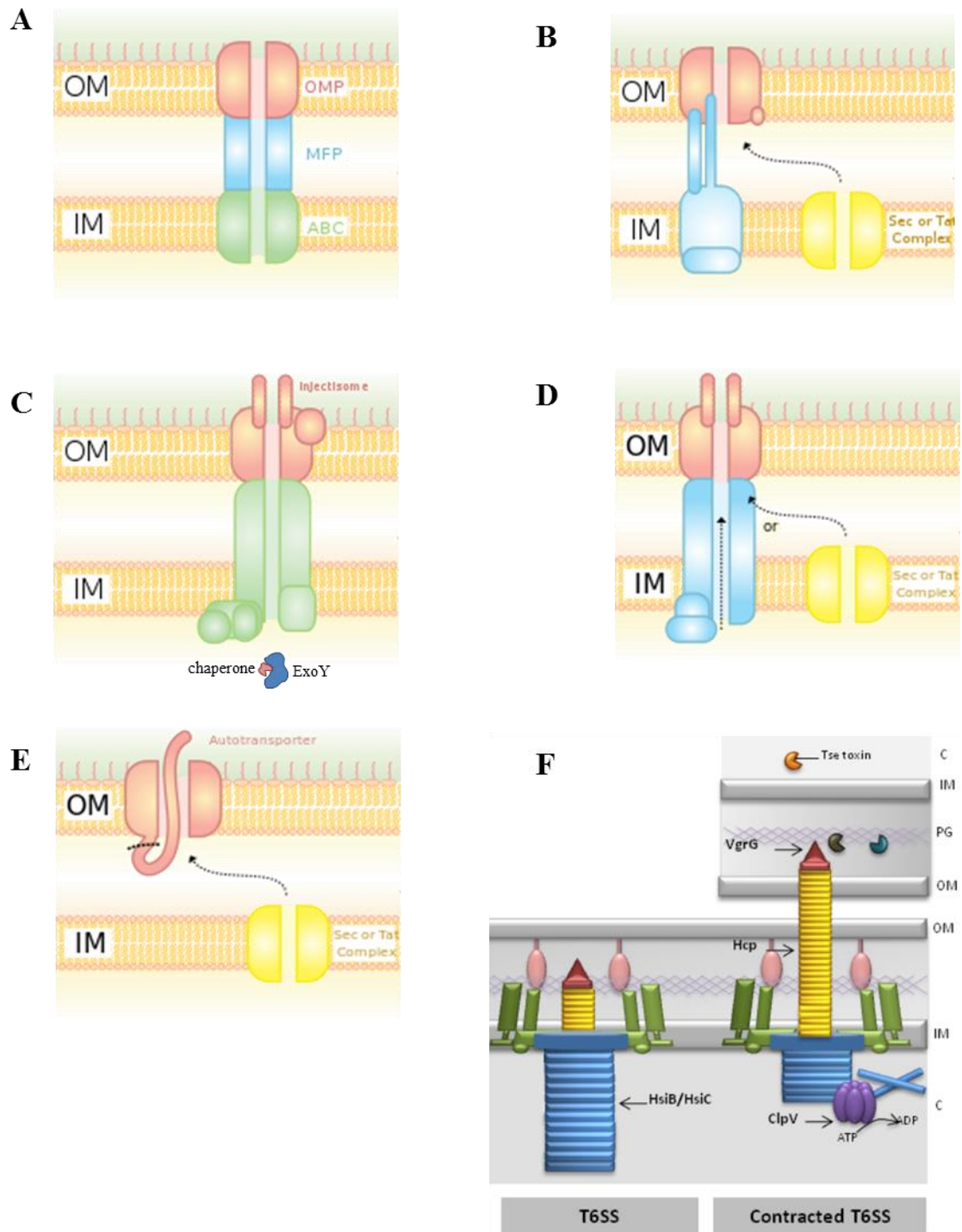


**Figure 1. Bacterial Secretion Systems.** **A)** Type 1 secretion system, **B)** Type 2 secretion system, which is Sec-dependent, **C)** Type 3 secretion system, which secretes *P. aeruginosa*'s effectors, including ExoY, **D)** Type 4 secretion system, **E)** Type 5 secretion system, which is also Sec-dependent, **F)** Type 6 secretion system. Panels **A – E** adapted from artwork by Mike Jones (adenosine) under the Creative Commons Attribution-Share Alike 3.0 Unported license. Panel **F** adapted from Filloux, A. (2013). The rise of the Type VI secretion system. *F1000prime reports*, 5(52).

envelope: an outer membrane protein (OMP), an ATP-binding cassette (ABC), and a membrane fusion protein (MFP), which assemble upon recognition of the ABC protein by the C-terminal secretion signal on the unfolded substrate [50, 51]. *Escherichia coli* hemolysin HlyA is a substrate of the T1SS [51].

The Type 2 Secretion System (T2SS) (Figure 1B) secretes fully-folded substrates through a pore composed of a complex of secretin proteins after the substrates are transported into the periplasmic space by the Sec or Tat complex [33]. The T2SS is found in Gram-negative bacteria, most notably in *Pseudomonas*, *Klebsiella*, and *Vibrio* [52]. The T2SS is used to secrete *Vibrio cholerae*'s cholera toxin (CT) as well as *P. aeruginosa*'s Exotoxin A [32, 52].

A prominent mechanism of pathogenicity for *P. aeruginosa* is the use of a Type 3 Secretion System (T3SS) (Figure 1C) to secrete effector proteins directly into the cytoplasm of eukaryotic cells during an infection [53]. The T3SS includes an injectosome, a needle-like structure found in many Gram-negative bacteria, including *Yersinia pestis* and *Salmonella typhimurium* [54], and the basal body, a structure that shares homology with the flagellar basal body [54]. Unlike the flagellum, however, the T3SS secretes pore-forming proteins to produce a pore, or translocon, in the host cell membrane [54]. This translocon formation in complex with the needle structure results in a direct channel between the bacterial cytosol and host cell cytosol, enabling the translocation of bacterial effector proteins directly into the host cells.

The Type 4 Secretion System (T4SS) (Figure 1D) is homologous to bacterial conjugation machinery [55], and is capable of transporting both DNA and protein directly into the host cell through a complex of proteins that spans the cell envelope [55, 56].

*Bordetella pertussis* utilizes the T4SS to secrete pertussis toxin direct into the cytosol of the host cell [56].

The Type 5 Secretion System (T5SS) (Figure 1E) is one of the most widely distributed secretion systems [57], utilizing the Sec system to cross the inner membrane. The  $\beta$ -barrel secondary structure of the substrate's C-terminus inserts into the outer membrane, and the N-terminal domain is allowed to go through the  $\beta$ -barrel. The N-terminus is then cleaved and enters the environment [58]. Notably, *Haemophilus influenzae* secretes its Hap adhesion/protease through the T5SS [58].

Finally, the Type 6 Secretion System (T6SS) (Figure 1F) has been recently identified in *V. cholerae* and *P. aeruginosa* [59, 60]. Subunits of the T6SS share homologies with subunits of the bacteriophage T4 tail spike and the current proposed mechanism of action suggests that the T6SS punctures the host cell membrane much like a bacteriophage [61–63].

### ***Pseudomonas aeruginosa* T3SS Regulation**

Induction of T3SS expression is under control of the ExsA regulatory cascade, which consists not only of ExsA, but also ExsD, ExsC, and ExsE (Figure 2). ExsA is a member of the AraC family of transcriptional activators that is activated upon contact with the eukaryotic cell or under reduced calcium concentrations. ExsD is capable of binding to and inhibiting ExsA, while ExsC can bind to and inhibit ExsD activity. ExsE inhibits ExsC and is also secreted by the T3SS. Under increased calcium concentrations, ExsE is not secreted and binds to ExsC. Because ExsC is unavailable, it cannot inhibit

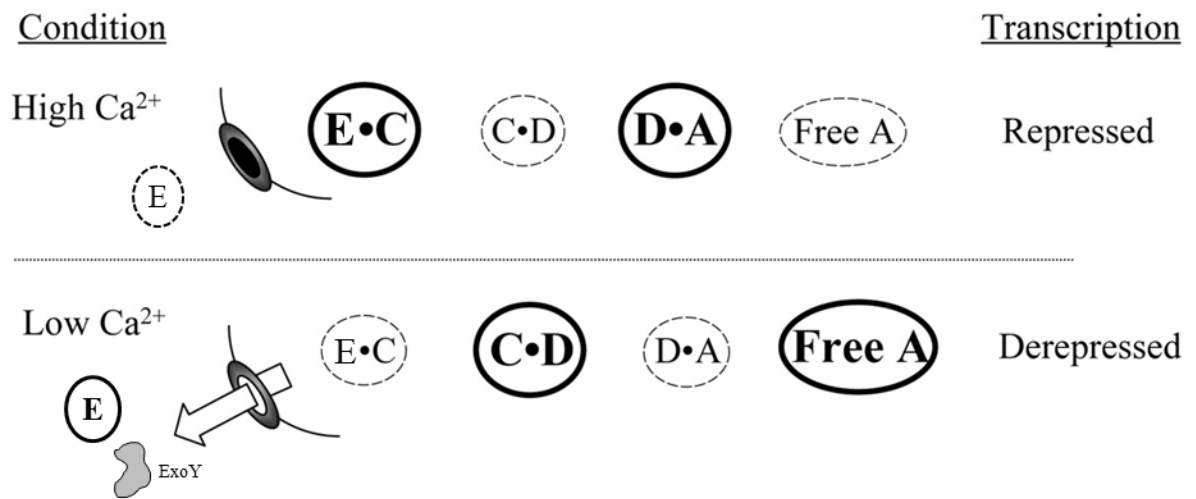


**Figure 2. ExsA Regulatory Cascade.** Under high Ca<sup>2+</sup> conditions, ExsE is not secreted and sequesters ExsC, allowing ExsD to repress ExsA, preventing transcription of the T3SS. Under low Ca<sup>2+</sup> conditions, ExsE is secreted along with *P. aeruginosa*'s effectors, including ExoY. ExsC sequesters ExsD, allowing ExsA to activate transcription of the T3SS. Image adapted from Urbanowski, Mark L. (2005). A secreted regulatory protein couples transcription to the secretory activity of the *Pseudomonas aeruginosa* type III secretion system. *Proceedings of the National Academy of Sciences of the United States of America*, 102(28),9930-9935.

ExsD, which binds to ExsA, blocking transcription. When the calcium concentration is lowered, however, ExsE is secreted by the T3SS, which releases ExsC, sequestering ExsD, and making ExsA available to activate T3SS transcription [64, 65].

### ***Pseudomonas aeruginosa* T3SS Effector Proteins**

#### **ExoU**

ExoU is the most cytotoxic effector protein secreted by *P. aeruginosa*'s T3SS – as few as 300 – 600 molecules of ExoU are enough to kill a mammalian host cell [66]. It functions as a broad-specificity phospholipase A2 (PLA<sub>2</sub>) and lysophospholipase, and is believed to break down the intoxicated cell's plasma membrane [67, 68]. ExoU is activated by the host cell's ubiquitin and ubiquitinated proteins [69].

#### **ExoS**

ExoS is a bifunctional enzyme with Rho GTPase-activating protein (GAP) and ADP-ribosyltransferase activity [70, 71]. As a Rho GAP, ExoS targets the actin cytoskeleton of the eukaryotic host cell, which results in the depolymerization of actin microfilaments [70]. Downstream, this can inhibit phagocytosis of *P. aeruginosa* during the immune response. As an ADP-ribosyltransferase, ExoS ADP-ribosylates Ras-signaling molecules, interfering with cell growth and division and ultimately leading to cell death [72]. Just behind ExoU, ExoS is the most cytotoxic of the effector proteins [73, 74]. Interestingly, ExoS and ExoU are mutually exclusive and rarely are the toxins expressed in the same bacterium [75]. ExoS is activated by a eukaryotic factor designated factor activating ExoS (FAS), which is a member of the 14-3-3 protein family [76], a

group of highly conserved proteins that have approximately 200 different identified binding partners [77].

### **ExoT**

Like ExoS, ExoT is a bifunctional enzyme with Rho GAP and ADP-ribosyltransferase activity [78, 79]. The Rho GAP function targets the actin cytoskeleton of the eukaryotic host cell, which results in the depolymerization of actin microfilaments [70], inhibiting the phagocytosis of *P. aeruginosa* during the immune response. Unlike ExoS, however, ExoT ADP-ribosylates the Crk family of proteins, an effect that also inhibits phagocytosis through uncharacterized means [79]. Like ExoS, ExoT is activated by a member of the 14-3-3 protein family [80]. ExoT is found in all strains of *P. aeruginosa*, although it exhibits the greatest contribution to infection when a strain secretes both ExoT and ExoS [81].

### **ExoY**

As an adenylyl cyclase, ExoY converts adenosine triphosphate (ATP) to cyclic-adenosine monophosphate (cAMP), an important secondary messenger utilized in many biochemical pathways such as glucose and lipid metabolism [82]. cAMP is perhaps best known for its ability to activate Protein Kinase A. This activation can have a variety of downstream effects, including lipolysis, glycogenolysis, and vasodilation [83–85]. Recently, ExoY has been shown to have generic nucleotidyl cyclase activity, with a strong preference for cyclic guanosine monophosphate (cGMP) and cyclic uridine monophosphate (cUMP) production [86]. Like cAMP, cGMP is a secondary messenger,

playing a role in phototransduction in the human eye, signal transduction in olfactory sensory neurons, and activation of protein kinases [87, 88]. cUMP, however, has not been well-characterized.

Previous work with infection models revealed that, when intoxicated with ExoY, Chinese hamster ovary (CHO) cells round off [89] and a pulmonary endothelial cell monolayer forms spaces between cells, similar to edema [90]. These observations, as well as the evidence indicating that the ExoY-produced cAMP stimulates Tau phosphorylation [91], which impairs microtubule growth, indicate the involvement of host cytoskeletal elements. It also chronically impairs cell proliferation and migration [92]. Nonetheless, these studies have been primarily performed *in vitro* – *in vivo* work is necessary to fully understand the contribution of ExoY to *P. aeruginosa* infections.

Other class II bacterial adenylyl cyclase effectors, such as Edema Factor (EF) of *Bacillus anthracis* or CyaA of *Bordetella pertussis*, are activated by calmodulin, a ubiquitous calcium-binding protein that functions as a secondary messenger in pathways involved in chemotaxis, muscle contraction, and glycogen metabolism [93]. Calmodulin interacts with CyaA and EF in different ways: the “open” conformation of calmodulin interacts with four different regions in CyaA to induce a conformational change, while the “closed” conformation binds to EF to induce activity [94–96]. Calmodulin has no effect on ExoY, since ExoY does not contain a calmodulin-binding domain; rather, ExoY requires activation by a non-calmodulin eukaryotic factor, the identity of which is currently unknown [97]. The goal of this research was to identify the eukaryotic activator of ExoY.

## Significance

Although ExoY is the least cytotoxic of *P. aeruginosa*'s T3SS effector proteins, there is evidence that it contributes to the virulence of *P. aeruginosa* during an infection [73, 81, 92, 98]. In tissue culture, ExoY causes cell rounding and gap formation [90, 97], which may improve the motility of *P. aeruginosa* through the tissues of the host during the establishment of an infection. In a 2014 study, after infection with *P. aeruginosa* that only expressed ExoY, a culture of pulmonary microvascular endothelial cells were unable to repair gaps [92]. Consequently, ExoY may not only play a role in the establishment of an infection, but it may also be responsible for prolonging an infection.

Other Class II bacterial adenylyl cyclase effectors such as Edema Factor (EF) of *Bacillus anthracis* and CyaA of *Bordetella pertussis* are activated by calmodulin [99–101], but the activity of ExoY is not affected by calmodulin. By understanding how ExoY is activated by a eukaryotic factor, not only can its role in pathogenesis be further defined, but it may also change the way the bacterial adenylyl cyclase effectors are classified.

## CHAPTER II: METHODS

### Cloning and Mutagenesis

Genomic DNA was extracted from *P. aeruginosa* ATCC 27853 [102] using the Puregene Genomic DNA Purification Kit (Gentra Systems, Minneapolis, MN) as per the manufacturer's instructions. The *exoY* gene (1.2 kbp) was amplified by polymerase chain reaction (PCR) using Taq polymerase (Invitrogen, Carlsbad, CA), custom primers (Integrated DNA Technologies, Coralville, IA; Table 1) designed to add 5'-NheI and 3'-EcoRI restriction sites to the *exoY* PCR product. The PCR product was resolved on a 0.7% (w/v) agarose gel and stained with ethidium bromide (1 µg/ml). The ~1.2 kbp product was extracted from the agarose gel using the QIAquick gel extraction kit (Qiagen, Valencia, CA) and concentrated by NaCl/EtOH precipitation. Mutagenesis primers (ExoYK81MFor and Rev) were designed to mutagenize lysine-81 (AAG) to methionine (ATG) using the XL QuickChange II Site-Directed Mutagenesis Kit (New England Biolabs, Ipswich, MA) as per the manufacturer's instructions (Table 1).

The *exoY* PCR product (1.2 kbp) was subjected to digestion with the NheI restriction endonuclease (New England BioLabs, Ipswich, MA) overnight at 37°C. The reaction contents were resolved on a 0.7% agarose gel, DNA excised, and extracted using the QIAquick gel extraction kit. This procedure was repeated with the EcoRI restriction endonuclease (New England BioLabs, Ipswich, MA) to produce a PCR product with sticky ends. This sequential digestion procedure was used to linearize the pET28 expression vector (5.4 kbp). The purified *exoY* PCR product was ligated in the purified pET28 with T4 DNA ligase (Fisher, Waltham, MA) according to the manufacturer's protocol. The product of the ligation reaction (pET28*exoY*) was transformed into

Table 1. Primer Characteristics

Name	Sequence (5' → 3')	Characteristics
ExoYForNheI	GGAGCTAGCATGCGTATCGACGGGTCATCGT	NheI
ExoYRevEcoRI	GGCGGAAATTCAGACCTTACGTTGGAAAAAGTC	EcoRI
T7F	ATTAATACGACTCACTATAGGG	
T7R	GCTAGTTAATTGCTCAGCGG	
ExoYK81MFor	CGCTGATCGAAGAGGGTTTCCCGACCA <u>TGGGCTTCTCGGTGAAGGGGAAAAAGCTC</u>	AAG → ATG
ExoYK81MRev	GAGCTTTTCCCTTCCACCAGAAAGCCCA <u>TGGTCGGGAAACCCTCTTCGATCAGCG</u>	CTT → CAI (reverse complement)

\* underlined nucleotides indicate location of primer characteristics

chemically competent DH5 $\alpha$  *E. coli* using standard methods. Transformants were selected on solid lysogeny broth (LB) containing kanamycin (0.05 mg/ml). Colonies that grew in the presence of kanamycin were presumed to harbor the pET28*exoY* plasmid. To verify the clone, the plasmid was isolated and the *exoY* insert was sequenced using the T7F and T7R primers (Table 1). Sequences were translated and analyzed by Basic Local Alignment Search Tool (BLAST, Table 2). The transformant with the *exoY* sequence matching the accepted literature sequence (NCBI: WP\_016263503.1) was streaked out on LB<sub>kan</sub>, plasmid purified, and transformed into the *E. coli* expression strain BL21.

### **Expression of recombinant ExoY (rExoY)**

BL21 pET28*exoY* was cultivated overnight in 10 ml LB<sub>kan</sub> at 37°C with shaking. The overnight culture was subcultured in 100 ml LB<sub>kan</sub> (1:50 dilution) and incubated for approximately 2 hours at 30°C with shaking. To induce rExoY expression, 1 mM isopropyl  $\beta$ -D-1-thiogalactopyranoside (IPTG) was added to the culture and incubated at 16°C with shaking overnight. The culture was subjected to centrifugation at 10,000 x g for 10 minutes to sediment the cells, the supernatant removed, and cells stored at -80°C. Cells were suspended in Bacterial Protein Extraction Reagent (B-PER; 4 ml) (Thermo Scientific, Waltham, MA) and incubated for 10 minutes at room temperature, or processed by French press four times at 10,000 psi; subsequently, the lysate was subjected to centrifugation at 15,000 x g for 15 minutes to sediment the unbroken cells/large particles (the pellet) from the soluble cell lysate (the supernatant). The soluble cell lysate was passaged through a 0.22  $\mu$ m syringe filter to remove small particulates.

Table 2. Strains and Vectors

Name	Genotype/Relevant Characteristics	Source or Reference
<b>Strains</b>		
DH5 $\alpha$	<i>E. coli</i> F- $\Phi$ 80lacZ $\Delta$ M15 $\Delta$ (lacZYA-argF) U169 recA1 endA1 hsdR17 (rK <sup>-</sup> , mK <sup>+</sup> ) phoA supE44 $\lambda$ -thi-1 gyrA96 relA1	Kind gift from collaborator Michael Baldwin
BL21 (DE3)	<i>E. coli</i> F-ompT hsdSB (rB-mB-) gal dcm (DE3)	Kind gift from collaborator Michael Baldwin
ATCC 27853	<i>P. aeruginosa</i> Schroeter Migula	Kind gift from collaborator Susan Galindo
<b>Vectors</b>		
pET28	pBR322 origin, amp <sup>r</sup>	Novagen
pET28exoY	Contains the <i>exoY</i> gene between the NheI and EcoRI sites	This study
pET28exoYK81M	Contains the <i>exoY</i> K81M gene between the NheI and EcoRI sites	This study

## **Nickel Affinity Chromatography**

The processed soluble cell lysate was added to HisPur Ni-NTA resin (Thermo Scientific) and the flow-through collected. The resin was washed twice with approximately ten column volumes of wash buffer (20 mM Na<sub>2</sub>HPO<sub>4</sub>, 300 mM NaCl, 25 mM imidazole, pH 7.4). Bound material was eluted with elution buffer (20 mM Na<sub>2</sub>HPO<sub>4</sub>, 300 mM NaCl, 250 mM imidazole, pH 7.4) and eluate collected in 1 ml fractions. The elution fractions that contained rExoY were determined by SDS-PAGE, pooled, and dialyzed overnight at 4°C in dialysis buffer (6 mM MgCl<sub>2</sub>, 10 mM Tris HCl pH 8.6, 2 mM DTT, 250 mM NaCl) using a 10,000 kDa cutoff membrane (Millipore, Billerica, MA). The rExoY preparation was stored at -80°C in 15% glycerol (v/v).

## **rExoY Antigen Preparation**

To prepare rExoY for antibody production, the histidine tag was removed from the protein. rExoY was added to thrombin buffer (20 mM Tris, pH 8.4, 150 mM NaCl, 2.5 mM CaCl<sub>2</sub>, 2 mM DTT) and thrombin at a ratio of 50 U thrombin to 2.5 mg rExoY. The reaction was incubated overnight at 4°C with gentle shaking. The products were resolved by SDS-PAGE to verify cleavage.

To remove the thrombin, a 150 µl bed volume of p-aminobenzamidine resin (GE Healthcare) was equilibrated with 2 bed volumes of thrombin buffer and the digested rExoY was applied to the column. The flow-through was collected and passaged through the resin twice. Removal of the poly-histidine tags was accomplished by passage through HisPur Ni-NTA Resin (Thermo Scientific). A 300 µl bed volume was equilibrated with 2 bed volumes of equilibration buffer (20 mM Na<sub>2</sub>HPO<sub>4</sub>, 300 mM NaCl, 10 mM imidazole,

pH 7.4). The final p-aminobenzamidine column flow-through was applied to the HisPur Ni-NTA column, collected, and reapplied two additional times. HisPur Ni-NTA flow-through was subjected to SEC to further purify the digested rExoY.

### **SDS-PAGE and Western Blot Analysis**

SDS-PAGE was performed with 10 x 8 cm discontinuous polyacrylamide gels in running buffer (25 mM tris, 192 mM glycine, 0.1% SDS) using a Hoefer SE250 electrophoresis apparatus (stacking at 75 V and separating at 90 V). Upon completion, gels were fixed in fixing solution (50% methanol, 10% acetic acid) for 20 min, stained in Coomassie solution (fixing solution with 0.1% brilliant blue G-250) for 20 min, and non-specific Coomassie stain removed in de-stain solution (30% methanol, 10% acetic acid) overnight. Alternatively, gels were stained with silver as per the manufacturer's instructions (Thermo Scientific, Waltham, MA). SDS-PAGE gels intended for western analysis were rinsed in transfer buffer (25 mM Tris, 192 mM glycine, 20% methanol) in preparation for transfer to nitrocellulose. The transfer procedure was conducted at  $\leq 400$  mA for 1 hour at 4°C. Nitrocellulose membranes were blocked with 5% milk in tris-buffered saline and probed with primary antibody (Mu  $\alpha$ -histidine antibody, 1/2,500) overnight at 4°C. Membranes were rinsed with tris-buffered saline and probed with secondary antibody (Gt  $\alpha$ -Mouse antibody-HRP, 1/10,000) for 1 hour at RT, rinsed with tris-buffered saline, incubated in SuperSignal West Pico Chemiluminescent Substrate (Thermo Scientific), and signal visualized on a Bio-Rad VersaDoc 3000 Imager.

## Densitometry

The concentration of rExoY was calculated using densitometry. Bovine serum albumin (BSA; Thermo Fisher Scientific, Rockford, IL) of various concentrations was resolved by SDS-PAGE as a standard beside various volumes of the rExoY prep. The intensities of the bands were analyzed on the Bio-Rad VersaDoc 3000 Imager (Bio-Rad, Philadelphia, PA), a standard curve produced, and the rExoY concentration calculated.

## Cell Culture and Lysis

The A549 cell line is a human lung adenocarcinoma epithelial cell line and is commonly used in *Pseudomonas* infection tissue culture models. Stock cultures were stored in DMEM with 5% DMSO in liquid nitrogen. The A549 cell line was maintained in Dulbecco's Modified Eagle Medium (DMEM) with 10% fetal bovine serum (FBS) and 1x penicillin/streptomycin mixture. Cells were incubated in 75 cm<sup>2</sup> tissue culture flasks at 37°C with 5% CO<sub>2</sub> and split every 5-7 days. To split, the confluent monolayer was washed twice with phosphate-buffered saline (PBS) followed by a trypsin rinse (0.25% v/v) for 5 min at 37°C. The trypsin was neutralized with DMEM + 10% FBS and the cell suspension was subjected to centrifugation at 200 x g for 5 minutes to sediment the cells, the supernatant removed, and cells stored at -20°C. Frozen cells were thawed and suspended in cell lysis buffer (20 mM NaCl, 20 mM Tris pH 8.6, RNase A (10 µg/ml), DNase I (10 µg/ml), 1:100 Halt protease inhibitor cocktail without EDTA (Thermo Scientific). Cells were lysed by passage through a 22 gauge double needle at 4°C and subjected to centrifugation at 10,000 x g for 10 min followed by ultracentrifugation at 100,000 x g for 1 hour to collect the soluble and insoluble fractions.

### **Adenylyl Cyclase Activity Assay**

The fidelity of rExoY adenylyl cyclase activity was examined using an *in vitro* activity assay. rExoY (15 nM) was incubated at 30°C with A549 soluble cell lysate (10 µg) in reaction buffer containing 2 mM ATP, 2 mM DTT, 6 mM MgCl<sub>2</sub>, and 10 mM Tris pH 9.3 at a final volume of 100 µl. The final pH of the assay was determined to be between 8.3 and 8.6. The reaction was allowed to proceed for 30 min and quenched with EDTA (4 mM). The quenched reaction was boiled for 5 min and subjected to centrifugation at 13,000 x g for 5 min to sediment precipitated protein [103]. The cAMP-containing supernatant was collected and stored at -20°C or directly added to the Cyclic AMP Direct EIA. Reaction containing rExoY K81M served as the negative control.

### **Cyclic AMP Direct Enzyme Immunoassay**

The cAMP-containing supernatant was analyzed using the Cyclic AMP Direct EIA Kit (Arbor Assays, Ann Arbor, MI) according to the manufacturer's instructions. Briefly, primer solution was added to α-sheep antibody-coated wells of a 96 well plate. Samples and standards were added to their designated wells. Peroxidase-conjugated cAMP was added to each well followed by the addition of sheep α-cAMP antibody. The mixture was allowed to equilibrate at RT for 2 hours while shaking vigorously, followed by four washes with wash buffer. 3,3',5,5'-Tetramethylbenzidine (TMB), a peroxidase substrate, was added to each well and the reaction was allowed to proceed at RT for 30 min, after which hydrochloric acid was added to quench the reaction. Absorbance at 450 nm was recorded using a Bio-Tek Synergy HT Microplate Reader and a standard curve

was generated using the 4 parameter logistic nonlinear regression equation in Prism Graphpad, a standard sigmoidal dose-response curve that plotted log cAMP concentrations on the x-axis and absorbance on the y-axis.

### **Pull-Down Assay**

HisPur Ni-NTA resin (50  $\mu$ l bed volume) was added to two disposable columns and washed twice with 1 ml binding buffer (20 mM Na<sub>2</sub>HPO<sub>4</sub>, 300 mM NaCl, 10 mM imidazole, pH 7.4, 1 mM DTT). BSA (0.3 mg) was added to each column to block. The column was washed and rExoY (83.6  $\mu$ g) added to saturation and incubated for 5 min at room temperature before collecting flow-through. The flow-through was added back to the resin and the process was repeated. Resin was washed (20 mM Na<sub>2</sub>HPO<sub>4</sub>, 300 mM NaCl, 25 mM imidazole, pH 7.4) twice to remove unbound rExoY. Soluble A549 lysate (1.5 mg) was added to the resin in the presence of Halt protease inhibitor cocktail without EDTA and incubated for 1 hour at 4°C. The eluate was collected and added back to the resin for 30 min at 4°C. The resin was washed twice after which elution buffer (20 mM Na<sub>2</sub>HPO<sub>4</sub>, 300 mM NaCl, 250 mM imidazole, pH 7.4) was added to the resin to elute rExoY and putative binding partner. Laemmli sample buffer was added to the resin and boiled for 5 min to evaluate bound protein. Sample was collected at each step and resolved by SDS-PAGE.

### **Size Exclusion Chromatography**

To enrich for the activator, the A549 soluble lysate was subjected to size exclusion chromatography (SEC). A glass column was packed with ~180 ml of Sephacryl

S-200 HR resin (GE Healthcare, Little Chalfont, United Kingdom) and equilibrated with 20/20 buffer (20 mM Tris, pH 8.6, 20 mM NaCl). A volume of A549 soluble lysate equal to ~2% of the bed volume (~3.6 ml) was applied to the top of the column. Chromatography was performed by isocratic gravity flow and eluted fractions collected every 10 min at 4°C. The fractions were assessed for their ability to activate rExoY using the activity assay above and protein visualized by SDS-PAGE.

### **Anion Exchange Chromatography**

To further enrich for the activator, the SEC fraction with the highest activity was selected for anion exchange chromatography. A 100 µl bed volume of DEAE Sepharose Fast Flow resin (GE Healthcare, Little Chalfont, United Kingdom) was equilibrated with 20 mM Tris, pH 8.6. The SEC fraction was applied, resin washed, and bound proteins were eluted with increasing stepwise concentrations of NaCl (100, 250, 500, 1000 mM).

### **Proteinase K Digestion**

A549 soluble lysate was subjected to Proteinase K digestion. Optimal Proteinase K activity was determined in the presence or absence of sodium dodecyl sulfate (0.2%), 50 µl A549 soluble lysate (~350 µg), and varying concentrations of Proteinase K (0.005 to 0.1 µg/µl) in 20/20 reaction buffer. The reaction was performed at 60°C for 1 hour. The reaction was quenched with the addition of either 1.6 mM AEBSF (4-(2-aminoethyl)benzenesulfonyl fluoride hydrochloride) or 5.4 mM PMSF (phenylmethylsulfonyl fluoride).

## CHAPTER III: RESULTS

### Cloning and Expression of rExoY (K81M)

A ~1.2 kbp PCR product was amplified in a polymerase chain reaction using primers that flanked the *exoY* gene in *P. aeruginosa* ATCC 27853 (Figure 3). The vector pET28 and the *exoY* PCR product were digested with NheI and EcoRI to produce a ~5.4 kbp and a ~1.2 kbp fragment, respectively (Figure 4). The PCR product was ligated into the multiple cloning site of pET28, fusing an N-terminal six-histidine tag separated from *exoY* by a thrombin cleavage site. Using primers that flanked the multiple cloning site of pET28, the nucleotide sequence of *exoY* was verified, translated, and the resulting amino acid sequence was input into the BLAST database, which identified protein product WP\_016263503.1 (ExoY) as identical to the cloned ExoY protein encoded in pET28 (Figure 5).

In preparation for ExoY activity analysis, a recombinant ExoY negative control that lacked activity was produced. Based on Yahr et al., lysine at the 81 amino acid position is necessary for adenylyl cyclase activity [97]. Site-directed mutagenesis primers for this mutation were designed and the plasmid pET28*exoY* was subjected to mutagenesis to change lysine-81 to methionine-81 (Table 1). Sequence analysis confirmed the mutation (Figure 6).

To further verify these clones, rExoY production was induced with IPTG and the protein profile was analyzed directly by SDS-PAGE (Figure 7A). Western blot analysis using the  $\alpha$ -histidine antibody confirmed the expression and presence of rExoY (Figure 7B). Once verified, rExoY was isolated and purified.

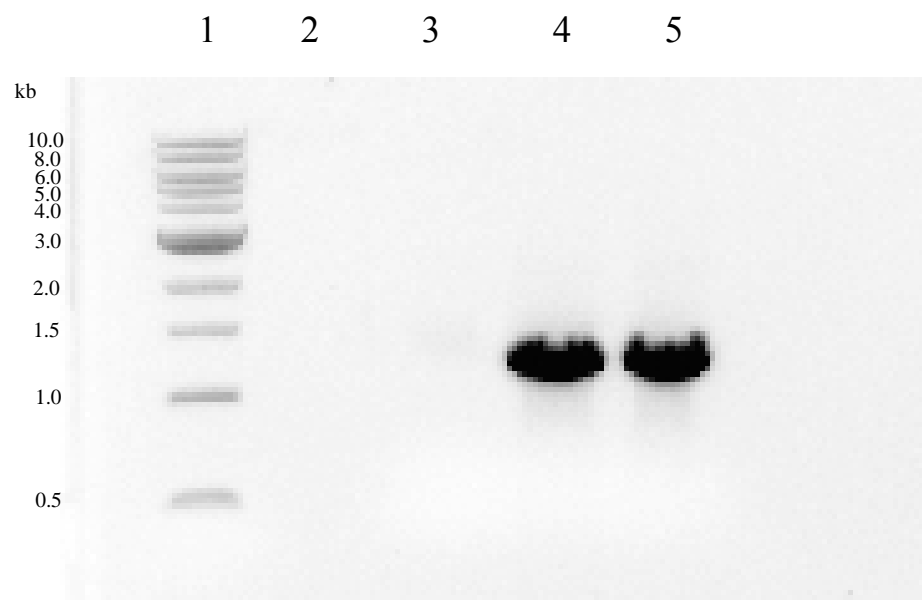


**Figure 3. Polymerase Chain Reaction *exoY* Gene Product.** Genomic DNA was extracted from *P. aeruginosa* ATCC 27853 and the *exoY* gene was amplified by PCR using primers that flanked the *exoY* gene. The products of the PCR reactions were resolved on a 0.7% agarose gel and stained with ethidium bromide. Lane 1: DNA ladder (kbp); Lanes 2 and 3: Amplified PCR product at ~1.2 kbp, the length of *exoY*.

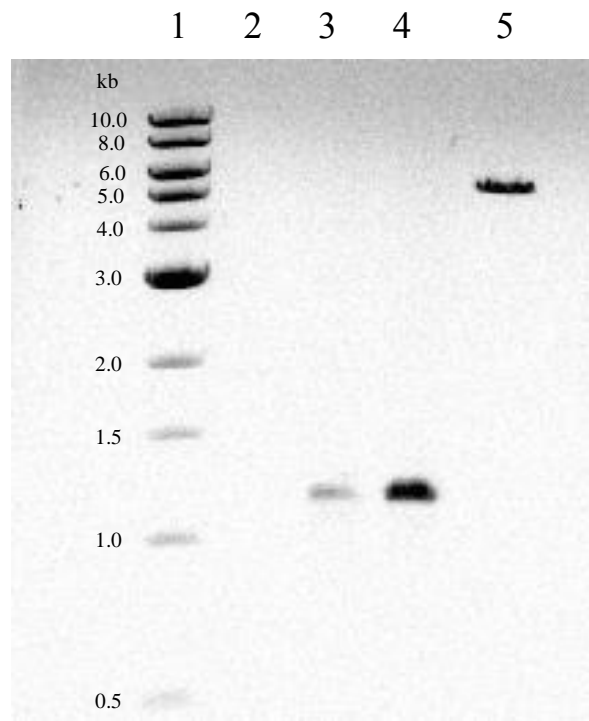


**Figure 4. Representative Ligation Products.** The *exoY* PCR product and the vector pET28 were subjected to *Nhe*I restriction endonuclease digest overnight at 37°C. Digestion products were resolved on a 0.7% agarose gel, and migrated at ~1.2 kbp and ~5.4 kbp for *exoY* and pET28 respectively. Lane 1: DNA ladder (kbp); Lanes 3 and 4: *exoY* *Nhe*I digestion products; Lane 5: pET28 *Nhe*I digestion products.

ExoY Sequence	1	MRIDGHRQVVSNATAQPGPLLRPADMQARALQDLFDAQGVGVPVEHALRMQAVARQTNTV	60
		MRIDGHRQVVSNATAQPGPLLRPADMQARALQDLFDAQGVGVPVEHALRMQAVARQTNTV	
Database	1	MRIDGHRQVVSNATAQPGPLLRPADMQARALQDLFDAQGVGVPVEHALRMQAVARQTNTV	60
ExoY Sequence	61	FGIRPVERIVTTLIEEGFPTKGFVSKGSSNWGPQAGFICVDQHLSKREDRDTAEIRKLN	120
		FGIRPVERIVTTLIEEGFPTKGFVSKGSSNWGPQAGFICVDQHLSKREDRDTAEIRKLN	
Database	61	FGIRPVERIVTTLIEEGFPTKGFVSKGSSNWGPQAGFICVDQHLSKREDRDTAEIRKLN	120
ExoY Sequence	121	LAVAKGMDGGAYTQDRLRISRQLAELVRNFGVLVADGVGVPVRLTAQGPSGKRYEFEARQ	180
		LAVAKGMDGGAYTQDRLRISRQLAELVRNFGVLVADGVGVPVRLTAQGPSGKRYEFEARQ	
Database	121	LAVAKGMDGGAYTQDRLRISRQLAELVRNFGVLVADGVGVPVRLTAQGPSGKRYEFEARQ	180
ExoY Sequence	181	EADGLYRISRLGRSEAVQVLASPACGLAMTADYDLFLVAPSIHAGSGGLDARRNTAVRY	240
		EADGLYRISRLGRSEAVQVLASPACGLAMTADYDLFLVAPSIHAGSGGLDARRNTAVRY	
Database	181	EADGLYRISRLGRSEAVQVLASPACGLAMTADYDLFLVAPSIHAGSGGLDARRNTAVRY	240
ExoY Sequence	241	TPLGAKDPLSEDFYGREDMARGNITPRTRQLVDALNDCLGRGEHREMFHHSDDAGNPGS	300
		TPLGAKDPLSEDFYGREDMARGNITPRTRQLVDALNDCLGRGEHREMFHHSDDAGNPGS	
Database	241	TPLGAKDPLSEDFYGREDMARGNITPRTRQLVDALNDCLGRGEHREMFHHSDDAGNPGS	300
ExoY Sequence	301	HMGDNFPATFYLPRAHEHRVGEESVRFDEVCCVADRKSFSLLVECIKNGYHFTAHPDWN	360
		HMGDNFPATFYLPRAHEHRVGEESVRFDEVCCVADRKSFSLLVECIKNGYHFTAHPDWN	
Database	301	HMGDNFPATFYLPRAHEHRVGEESVRFDEVCCVADRKSFSLLVECIKNGYHFTAHPDWN	360
ExoY Sequence	361	VPLRPGFQEALDFQQRKV*	378
		VPLRPGFQEALDFQQRKV	
Database	361	VPLRPGFQEALDFQQRKV*	378

**Figure 5. Translation of *exoY* Sequence.** Sequence data of the *exoY* gene was obtained via capillary sequencing and translated using pDRAW software. Translation was compared with the protein BLAST database using the BLOSUM62 matrix.

Plasmid sequence		MGSSHHHHHHSSGLVPRGSHMAS	
K81M Sequence	1	MRIDGHRQVVSNATAQPGPLLRPADMQARALQDLFDAQGVGVPVEHALRMQAVARQTNTV	60
		MRIDGHRQVVSNATAQPGPLLRPADMQARALQDLFDAQGVGVPVEHALRMQAVARQTNTV	
Database	1	MRIDGHRQVVSNATAQPGPLLRPADMQARALQDLFDAQGVGVPVEHALRMQAVARQTNTV	60
K81M Sequence	61	FGIRPVERIVTTLIEEGFPTM	120
		FGIRPVERIVTTLIEEGFPT	
Database	61	FGIRPVERIVTTLIEEGFPTK	120
K81M Sequence	121	LAVAKGMDGGAYTQDRLRISRQRLAELVRNFGVLVADGVGVPVRLTAQGPSGKRYEFEARQ	180
		LAVAKGMDGGAYTQDRLRISRQRLAELVRNFGVLVADGVGVPVRLTAQGPSGKRYEFEARQ	
Database	121	LAVAKGMDGGAYTQDRLRISRQRLAELVRNFGVLVADGVGVPVRLTAQGPSGKRYEFEARQ	180
K81M Sequence	181	EADGLYRISRLGRSEAVQVLASPACGLAMTADYDLFLVAPSIEAHGSGGLDARRNTAVRY	240
		EADGLYRISRLGRSEAVQVLASPACGLAMTADYDLFLVAPSIEAHGSGGLDARRNTAVRY	
Database	181	EADGLYRISRLGRSEAVQVLASPACGLAMTADYDLFLVAPSIEAHGSGGLDARRNTAVRY	240
K81M Sequence	241	TPLGAKDPLSEDFYGREDMARGNITPRTRQLVDALNDCLGRGEHREMFHHSDDAGNPGS	300
		TPLGAKDPLSEDFYGREDMARGNITPRTRQLVDALNDCLGRGEHREMFHHSDDAGNPGS	
Database	241	TPLGAKDPLSEDFYGREDMARGNITPRTRQLVDALNDCLGRGEHREMFHHSDDAGNPGS	300
K81M Sequence	301	HMGDNFPATFYLPRAHEHRVGEESVRFDEVCCVADRKSFSLLVECIKNGYHFTAHPDWN	360
		HMGDNFPATFYLPRAHEHRVGEESVRFDEVCCVADRKSFSLLVECIKNGYHFTAHPDWN	
Database	301	HMGDNFPATFYLPRAHEHRVGEESVRFDEVCCVADRKSFSLLVECIKNGYHFTAHPDWN	360
K81M Sequence	361	VPLRPGFQEALDFFQRKV*	378
		VPLRPGFQEALDFFQRKV	
Database	361	VPLRPGFQEALDFFQRKV*	378

**Figure 6. Translation of pET28 *exoYK81M* Sequence.** Sequence data of the *exoYK81M* gene was obtained via capillary sequencing and translated using pDRAW software. Translation was compared with the protein BLAST database using the BLOSUM62 matrix. The mutation is highlighted with a rectangle. Amino acid sequence of 5'-histidine tag is labeled 'plasmid sequence'.

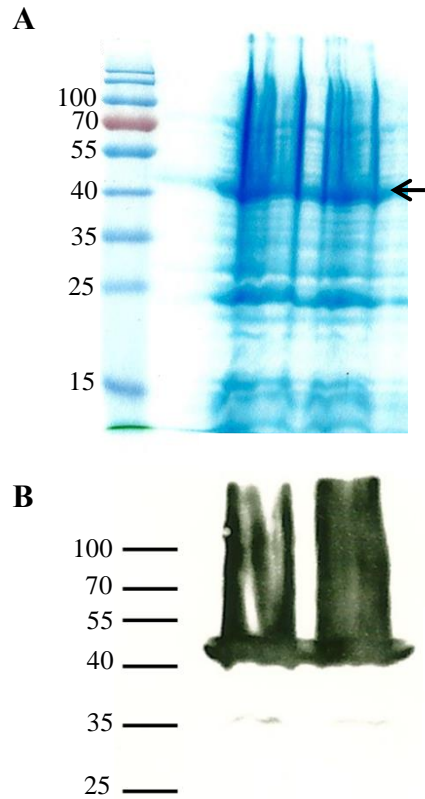


**Figure 7. Induction of Recombinant ExoY.** **A)** Two replicates of BL21 pET28b *exoY* whole cell lysates were resolved on a 10% SDS-PAGE gel and subsequent western blot (**B**). Arrow denotes probable location (42 kDa) of rExoY. **B)** Immunoblot probing BL21 pET28b *exoY* whole cell lysates with mouse  $\alpha$ -histidine primary antibody and donkey  $\alpha$ -mouse-HRP secondary antibody.

After a 15,000 x g centrifugation, the induced soluble lysate from BL21 pET28*exoY* lysate filtrate was loaded onto a column with HisPur Ni-NTA resin for purification. Bands at ~42 kDa were detected in Elutions 2 – 5 and Elutions 2 and 3 were pooled and dialyzed to remove imidazole (Figure 8A). An identical protocol was conducted to purify K81M from BL21 pET28*K81M* soluble lysate. Elutions 2 – 4 were pooled and dialyzed to remove imidazole (Figure 8B).

To quantify the amounts of the rExoY and K81M preps, we performed densitometry using BSA as a standard. The concentration of the rExoY prep was determined to be 0.76  $\mu\text{g}/\mu\text{l}$  (Figure 9A), while the K81M prep was calculated to be 0.577  $\mu\text{g}/\mu\text{l}$  (Figure 9B).

As the polyclonal  $\alpha$ -ExoY antibody recognized additional proteins, including the actual six-histidine tag fused to rExoY, a thrombin digestion was performed to remove the tag. The digestion products were applied to p-aminobenzamidine resin in a disposable column to remove thrombin, followed by application to HisPur Ni-NTA resin to collect the free poly-histidine tags or rExoY with the tag intact. rExoY was recovered from the benzamidine column, but after being subjected to the HisPur Ni-NTA resin, the recovery decreased dramatically (Figure 10A). rExoY without the tag appears to have an affinity for or gets stuck within the resin, preventing efficient recovery. Despite this, the recovered fractions were subjected to SEC to further purify the remaining rExoY (Figure 10B). These fractions were pooled and used to produce antibody to rExoY lacking the six-histidine tag.

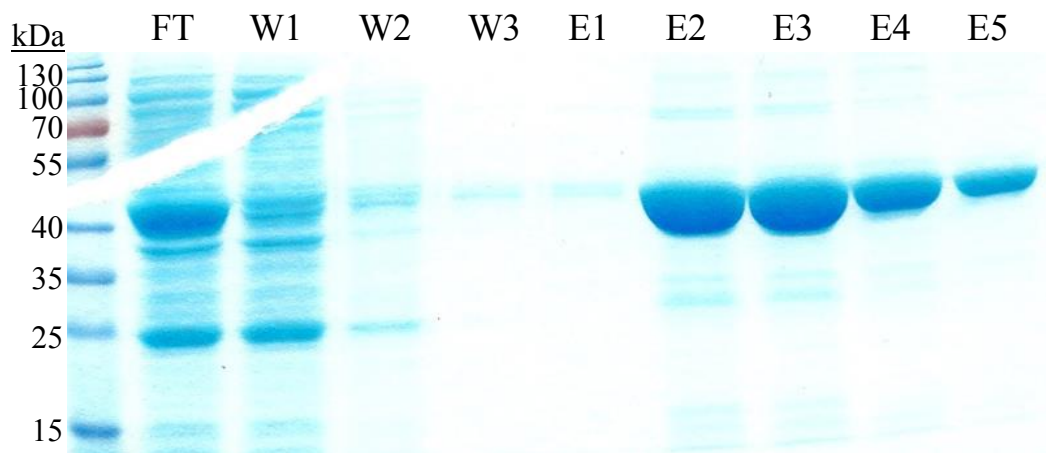


**Figure 8A. Recombinant ExoY Purification Scheme.** The BL21 pET28b *exoY* soluble lysate was passed through a 0.22  $\mu\text{m}$  syringe filter and the filtrate was loaded onto a HisPur Ni-NTA resin column. After three washes with wash buffer, rExoY was eluted from the column in five separate elution steps.

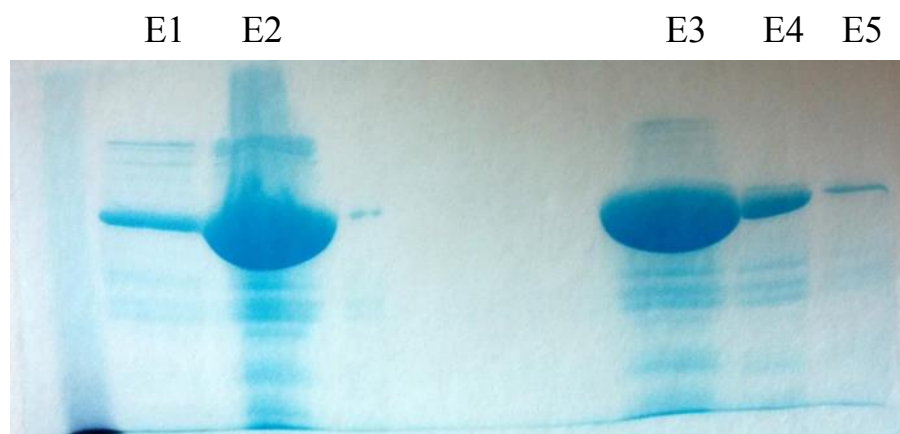


**Figure 8B. Recombinant ExoY K81M Purification Scheme.** The BL21 pET28b *exoYK81M* soluble lysate was passed through a 0.22  $\mu\text{m}$  syringe filter and the filtrate was loaded onto a HisPur Ni-NTA resin column. After three washes with wash buffer, rExoY (K81M) was eluted from the column in five separate elution steps. Only the eluted fractions are shown. Note – no ladder was added to the gel.

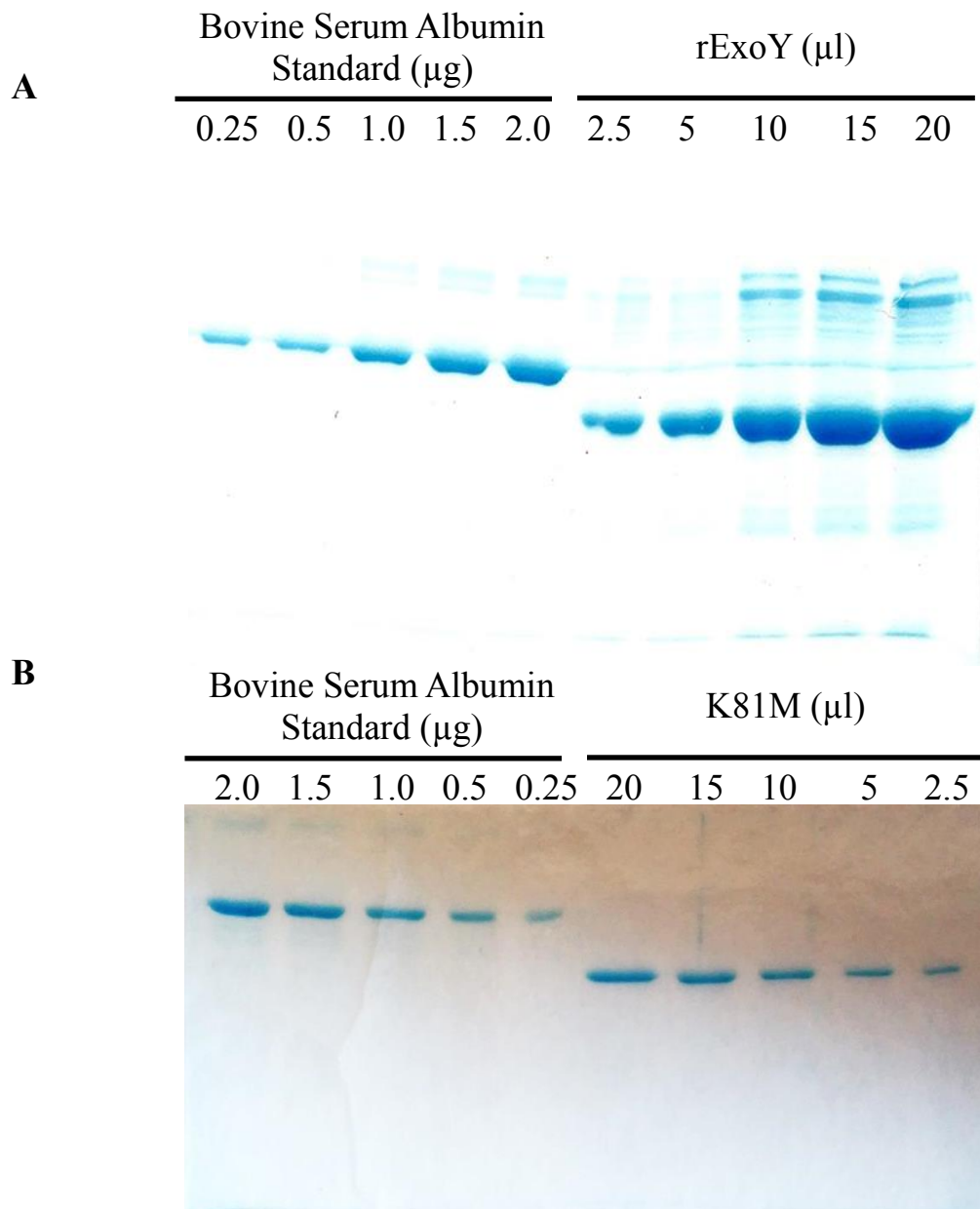


**Figure 9. Densitometric Quantification of rExoY (K81M).** A standard curve was constructed using known concentrations of bovine serum albumin stained with Coomassie blue and each protein band's densitometric load. The densitometric load of known volumes of rExoY (K81M) was compared to the standard curve to obtain protein concentration. **A)** rExoY **B)** rExoY K81M.

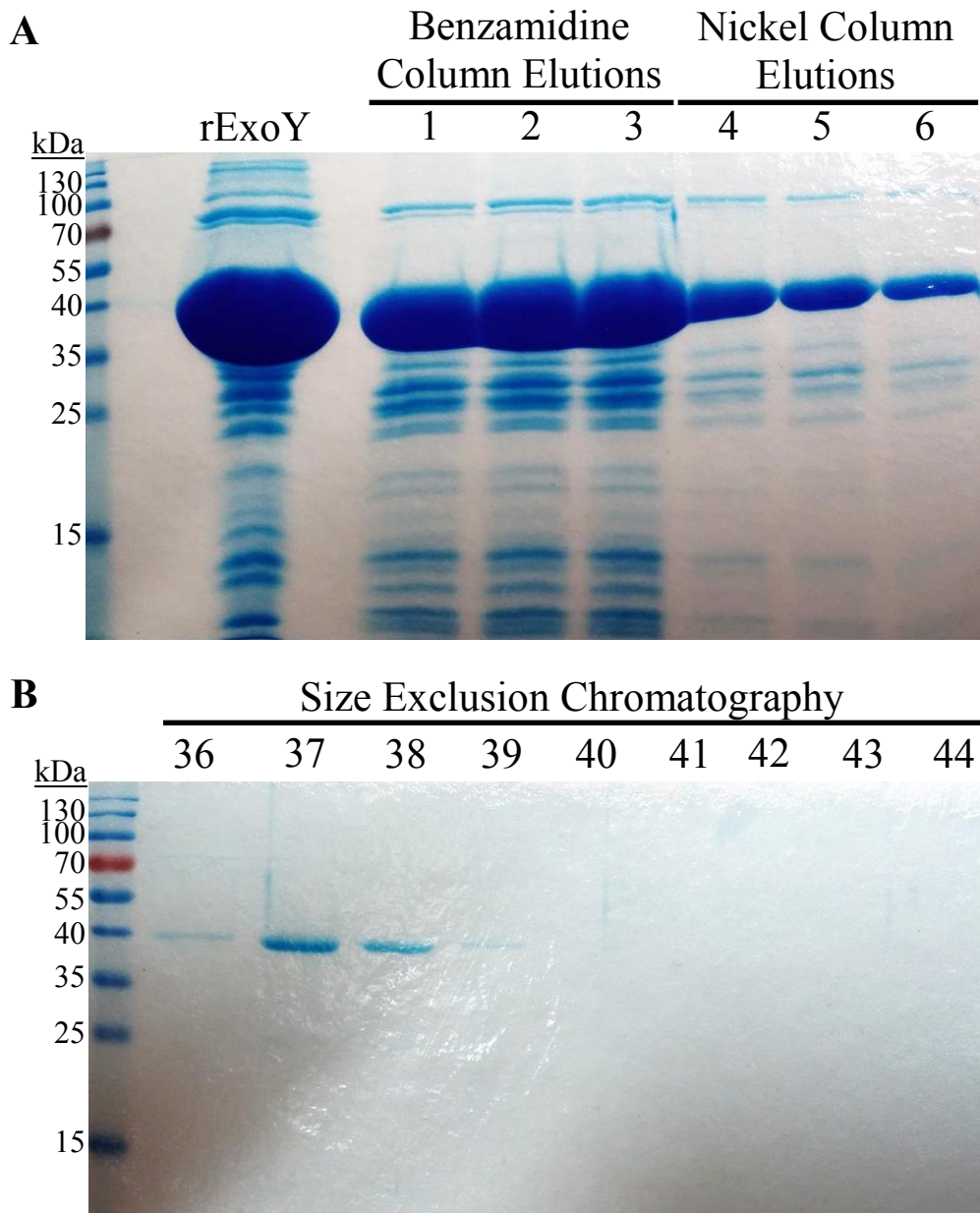


**Figure 10. Protein Profile of the Chromatography Steps Used to Prepare rExoY for Antibody Production.** **A)** The elution profile of thrombin-digested rExoY. The first lane represents the input. Elutions 1 - 3 depict the elution profile of rExoY passed through thrombin-binding benzamidine resin to capture thrombin. Elutions 4 - 6 depict the elution profile of rExoY passed through nickel resin to capture the free histidine tag. **B)** The protein profile of rExoY purified by size exclusion chromatography. Numbers depict fraction number.

## **Optimization of Cyclic AMP Direct EIA**

To interpret the results of the Cyclic AMP Direct EIA, every assay is accompanied by a set of cAMP standards. The standard curve fits to a 4 parameter logistic nonlinear regression equation (Figure 11).

Dithiothreitol (DTT) is a reducing agent used in the ExoY activity assay to prevent the five cysteines in rExoY from forming intra- and inter-protein disulfide bonds, which has been shown to cause aggregation and precipitation of rExoY [97]. Because our Cyclic AMP Direct EIA relies on antibodies for detection and quantification of cAMP, we were concerned that the presence of DTT in our samples would affect the results. To examine the effect of DTT on this assay, we performed this assay in the presence of varying amounts of cAMP (0 – 5 pmol) and DTT (0 – 2 mM). While 2 mM DTT did appear to affect the detection capabilities of the assay, 0.2 mM DTT did not differ from those reactions that lacked DTT (Figure 12). rExoY (5  $\mu$ l) containing 2 mM DTT was added to a final volume of 100  $\mu$ l in the activity assay, yielding a final DTT concentration of 0.1 mM. As this value is lower than our tested value of 0.2 mM, we determined that DTT (< 0.2 mM) did not affect the Cyclic AMP Direct EIA (Figure 12).

To examine the reliability and reproducibility of the assay system, we compiled the ExoY activity data from various replicates of the activity assay/Cyclic AMP Direct EIA and compared them to one another. Day-to-day variability was observed when a single individual performed the assay. The mean cAMP varied from 9017 pmol/ml to 25,185 pmol/ml (Figure 13). A student's t-test (unpaired) applied to the replicates performed between personnel reported a P value of 0.0589, indicating that the differences between individuals were not quite statistically significant.

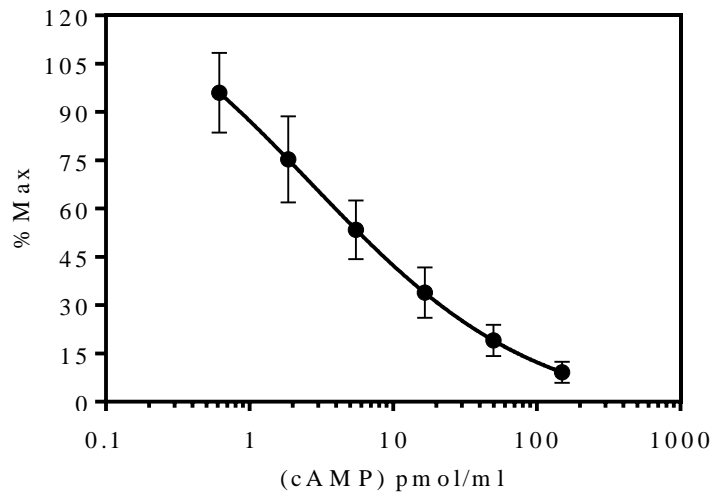


**Figure 11. Validation of the cAMP EIA Standard Curve.** cAMP standards (0.6, 1.9, 5.6, 16.7, 50, and 150 pmol/ml) for every assay were data fit to a 4 parameter logistic nonlinear regression equation (variable slope) to obtain a sigmoidal dose response curve. The data points represent the arithmetic mean and standard deviation of 18 individual experiments.  $R^2$  value = 0.9229.

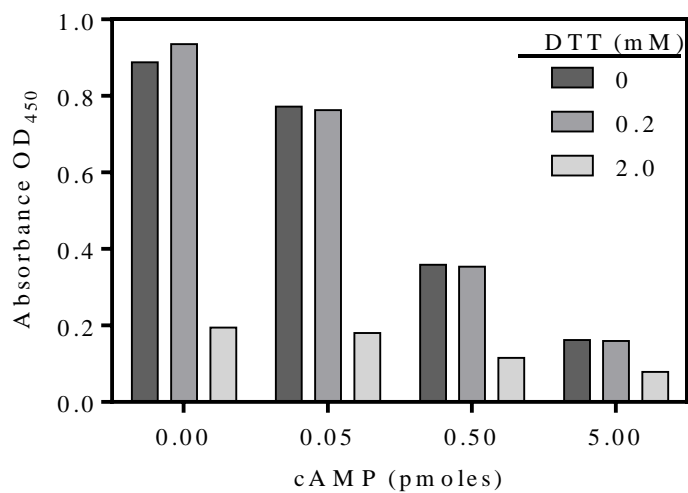


**Figure 12. Effect of Dithiothreitol (DTT) on the cAMP EIA.** To test the effect of DTT on the cAMP EIA, varying amounts of known cAMP standards (0.0, 0.05, 0.5, and 5 pmol) in the presence (0.2 mM or 2.0 mM) or absence of DTT was examined.

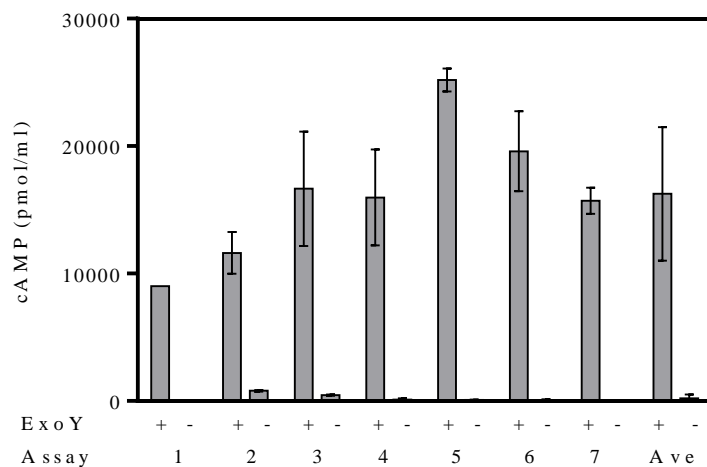


**Figure 13. Accuracy of the ExoY Activity Assay/cAMP EIA.** Reproducibility of the assays between days and among personnel is variable. Each set of columns (ExoY +/-) represents an assay performed. Error bars for each day represent the standard deviation of replicate data. The last column set represents the arithmetic mean and standard deviation for the seven independent assays.

## Biochemical Enrichment of the ExoY Activator

The six-histidine tag fused to rExoY is utilized during the purification process and for protein-protein interaction assays. As such, we utilized the HisPur Ni-NTA resin to immobilize rExoY as bait to capture the activator. Three putative ExoY binding partners captured from A549 soluble lysate were identified in the elution and resin fractions in the presence of rExoY, but not in its absence. These putative binding partners migrated at ~80, 28, and 15 kDa by SDS-PAGE (Figure 14). Immunoblotting with  $\alpha$ -rExoY antibody revealed that the 28 and 15 kDa proteins were contaminants within the rExoY prep and were eliminated as *bona fide* candidates (data not shown). Repeated pull-down assays did not show the ~80 kDa protein, indicating further optimization of the assay is necessary.

Size exclusion chromatography separated A549 soluble lysate proteins by size and fractions were assayed for their ability to activate rExoY (Figure 15). The specific activity of rExoY was greater in the early fractions of protein, which signified enrichment of the ExoY activator in those fractions. The A549 lysate proteins that were eluted in fraction 25 were subjected to anion exchange chromatography to separate the proteins based on charge. The protein profile for each elution appears to have subtle differences and a majority of the proteins were eluted by the third 500 mM NaCl elution (Figure 16). At this point, the proteins were barely visible on a Coomassie-stained gel, and we opted to repeat this enrichment step at a later time with higher amounts of starting material. After the A549 soluble lysate was subjected to ultracentrifugation to remove insoluble material, we observed a lipid film that remained on top of the supernatant. This film was assayed for the ability to activate rExoY and a level of activity similar to that of the soluble lysate was observed (Figure 17). When the ultracentrifugation pellet was

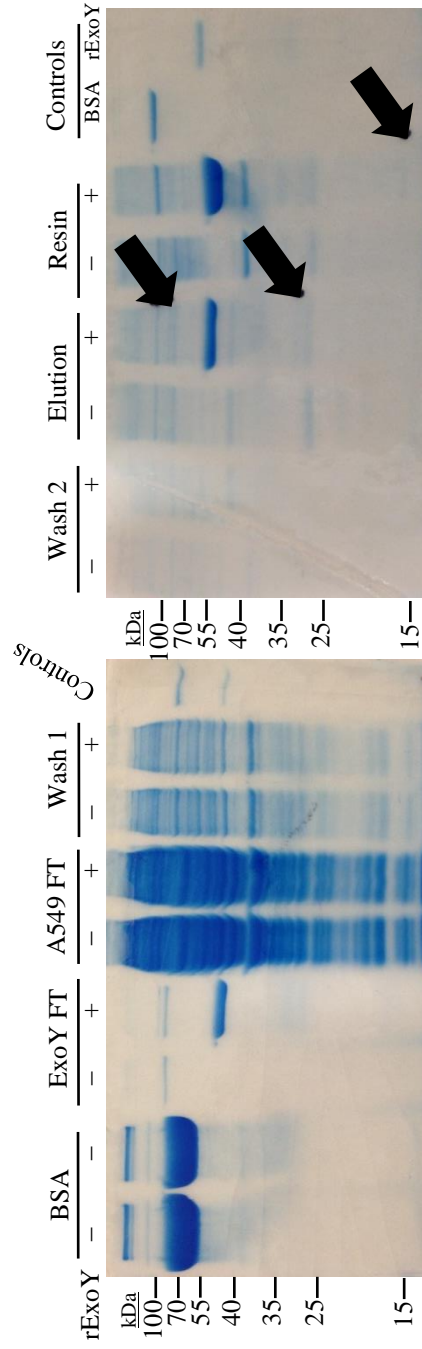


**Figure 14. Pull Down using rExoY as Bait and A549 Soluble Lysate as Prey Yielded Three Activator Candidates.** Two columns of HisPur Ni-NTA resin were blocked with BSA. rExoY was added to the 1<sup>st</sup> column; no rExoY was added to the 2<sup>nd</sup> column and served as the negative control (rExoY -). Soluble A549 lysate was added to each column and washed multiple times. Elution buffer was added to each column and the resin was collected to evaluate elution efficiency. The controls on the SDS-PAGE gels were BSA and rExoY. Arrows denote putative ExoY-binding protein (activator). FT = flow through.

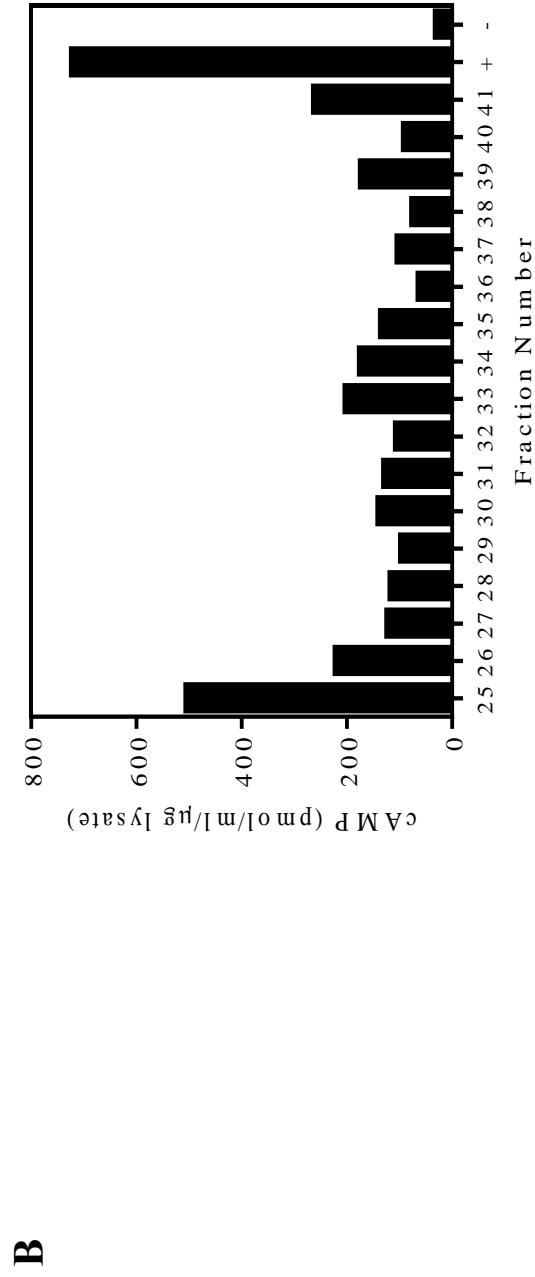
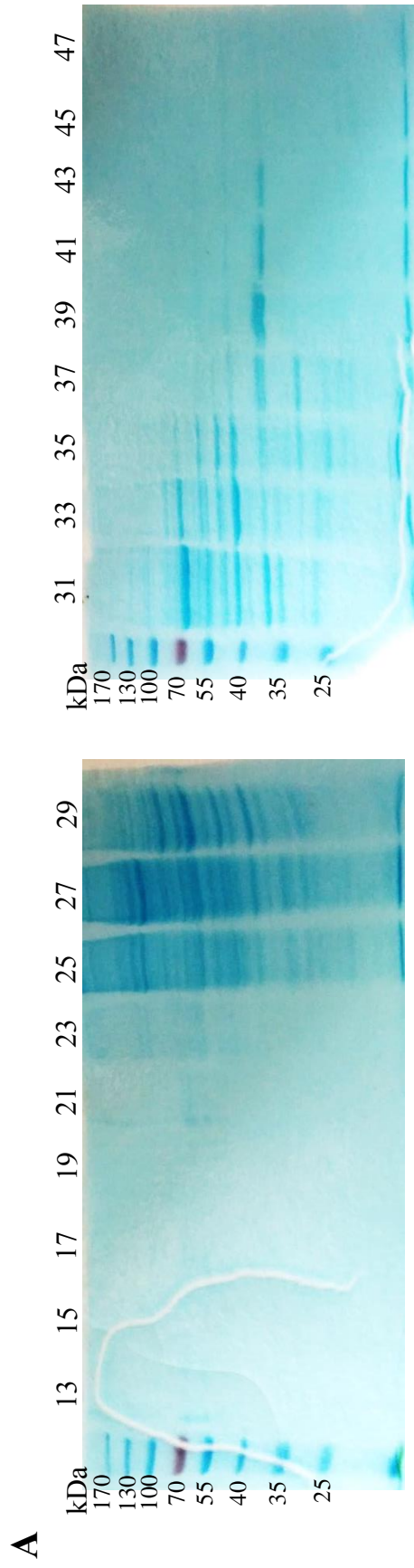


**Figure 15. Size Exclusion Chromatography A549 Protein Profile and rExoY Activity.** **A)** The A549 soluble cell lysate was subjected to size exclusion chromatography and the fractions resolved by SDS-PAGE. Numbers indicate fraction number. **B)** rExoY activity in the presence of size exclusion fractions 25 – 41. Values are reported in pmol cAMP ml<sup>-1</sup> µg lysate<sup>-1</sup>.

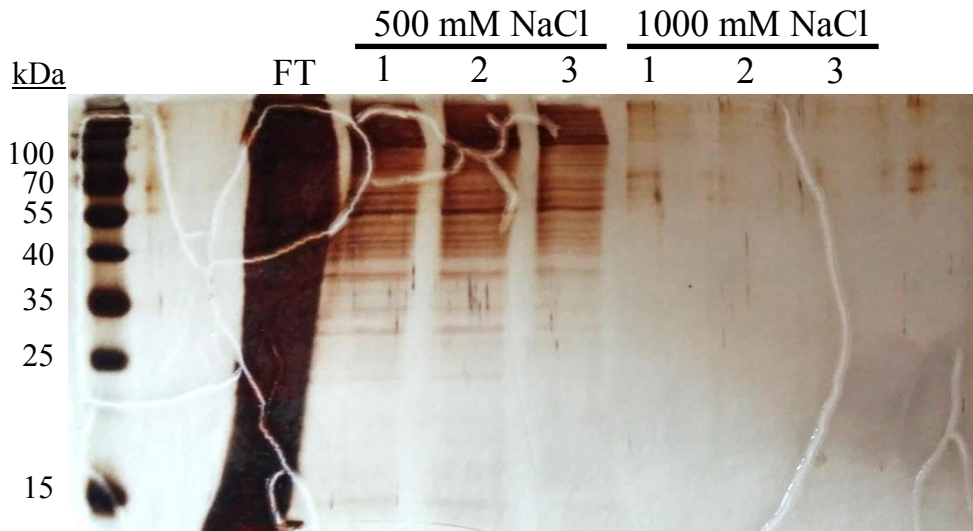
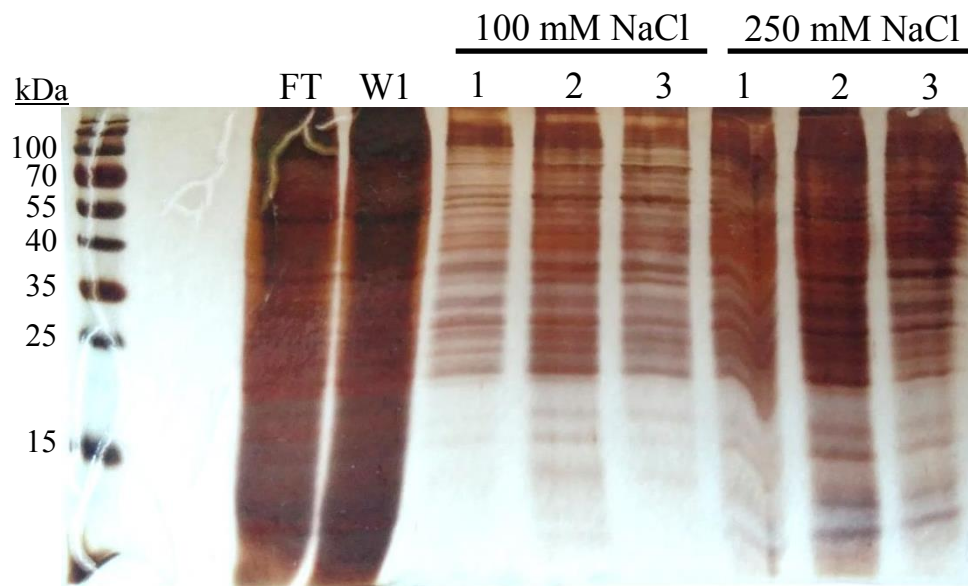


**Figure 16. Protein Profile of A549 Lysate Separated by Anion Exchange.** Fraction 25 (Figure 15) was subjected to anion exchange chromatography and the elutions resolved on SDS-PAGE and silver stained . FT = flow through, W = wash

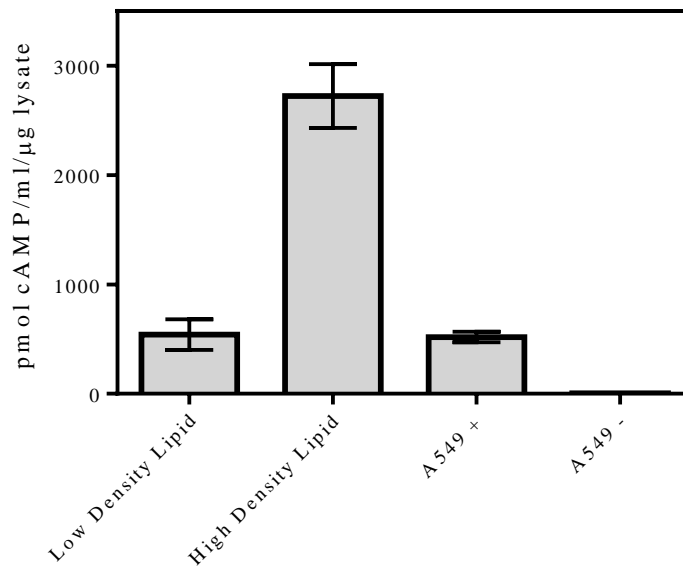


**Figure 17. rExoY-Mediated cAMP Production is Highest in the A549 High Density Lipid.** A549 cells were lysed and subjected to centrifugation at 20,000 x g for 20 min and the supernatant was subjected to ultracentrifugation at 100,000 x g for 1 hour. The resulting pellet was termed the high density lipid fraction and the floating content termed the low density lipid. The A549 supernatant after low speed centrifugation served as the adenylyl cyclase activity assay positive control and a reaction without A549 lysate served as the negative control. Data represent the arithmetic mean and standard deviation of two independent replicates.

assayed for rExoY activity, a level of cAMP production nearly five times that of the standard soluble lysate activity was observed (Figure 17).

As components in the A549 lipid pellet activated rExoY five times more than the soluble lysate, A549 was digested with Proteinase K to determine if the activator was proteinaceous. A protocol was planned to subject A549 soluble lysate to a Proteinase K digestion, however, to prevent digestion of rExoY in the activity assays, the digestion procedure had to be optimized. The manufacturer's protocol for Proteinase K suggested that 1% SDS would be necessary to promote activity; however, the presence of SDS could have affected downstream steps for cAMP production and detection. The Proteinase K digestion of the A549 soluble lysate was performed with and without 0.2% SDS. Both reactions were successful in digesting the A549 soluble lysate and SDS was eliminated from the protocol (Figure 18).

To determine the optimal concentration of Proteinase K that digested lysate, various concentrations (0.005  $\mu\text{g}/\mu\text{l}$  – 0.1  $\mu\text{g}/\mu\text{l}$ ) were tested in separate digestion reactions. Based on the protein profile of the digestion reactions, a Proteinase K concentration of 0.025  $\mu\text{g}/\mu\text{l}$  was selected for all future digestions (Figure 19).

The 4-(2-Aminoethyl) benzenesulfonyl fluoride hydrochloride (AEBSF)-containing Halt protease inhibitor cocktail was examined for its ability to inhibit Proteinase K activity. Varying dilutions of protease inhibitor cocktail (1:12.5 – 1:200, equivalent to 0.625  $\mu\text{g}$  – 10  $\mu\text{g}$  AEBSF) were used to quench the digestion of A549 lysate by Proteinase K (0.025  $\mu\text{g}/\mu\text{l}$ ). The protein profile demonstrated that the protease inhibitor cocktail failed to prevent digestion of rExoY at any dilution (Figure 20).

Pure AEBSF was purchased and its efficacy of activity as a Proteinase K inhibitor

Proteinase K	-	+	+
SDS	-	+	-



**Figure 18. Effect of Sodium Dodecyl Sulfate (SDS) on Proteinase K Activity.** Proteinase K activity increases in the presence of SDS. To verify whether or not SDS was required for Proteinase K activity, the Proteinase K digestion of the A549 soluble lysate was performed with 50  $\mu$ l soluble lysate (~325  $\mu$ g), 0.1  $\mu$ g/ $\mu$ l Proteinase K, and either 0.2% SDS or a reaction lacking SDS. The digestion reaction was incubated at 60°C for 1 hour and the products resolved on a 13% SDS-PAGE gel.

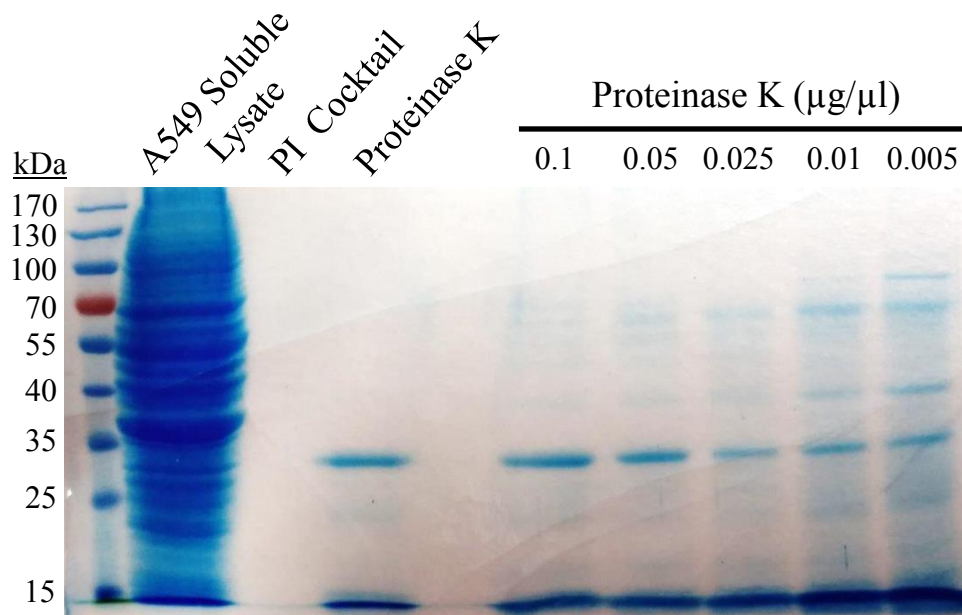


**Figure 19. Optimal Concentration of Proteinase K for the A549 Digestion Reaction.** Varying concentrations of Proteinase K (0.005  $\mu\text{g}/\mu\text{l}$  – 0.1  $\mu\text{g}/\mu\text{l}$ ) were used to digest 40  $\mu\text{l}$  soluble lysate (~ 300  $\mu\text{g}$ ) in the presence of 20/20 buffer at 60°C for 1 hour. Control lanes include undigested soluble A549 lysate, the PI (protease inhibitor) cocktail used to quench the reaction, and Proteinase K alone (0.1  $\mu\text{g}/\mu\text{l}$ ). Protein was analyzed by 10 % SDS-PAGE.

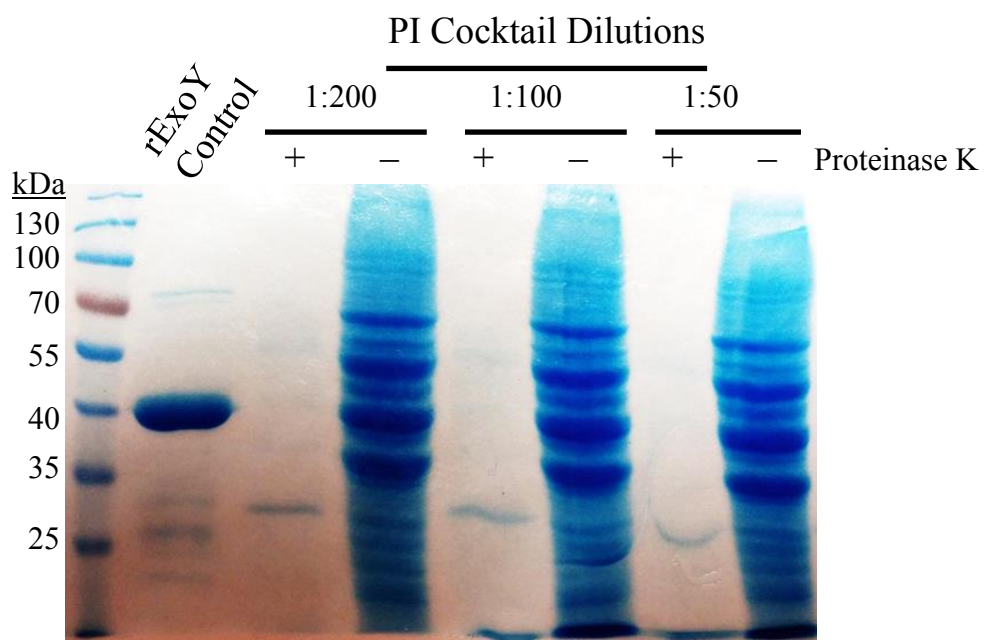


**Figure 20. Effects of the Protease Inhibitor Cocktail on Proteinase K.** Varying dilutions of protease inhibitor cocktail (1:12.5 – 1:200) were used to quench the digestion of soluble A549 lysate (150  $\mu\text{g}$ ) in the presence of 0.025  $\mu\text{g}/\mu\text{l}$  Proteinase K and 20/20 buffer at 60°C for 1 hour. 6  $\mu\text{g}$  of rExoY was added to the reaction and allowed to incubate at 30°C for 30 minutes. rExoY served as the loading control. Protein was analyzed by 10 % SDS-PAGE.

was examined. The protein profile of the reaction products revealed that AEBSF did not inhibit Proteinase K digestion of rExoY or the control protein, BSA (Figure 21A). The failure of AEBSF as a Proteinase K inhibitor caused us to turn our attention to a different serine protease inhibitor, phenylmethanesulfonylfluoride (PMSF, 1.8 mM). The same control reactions were performed, and the protein fingerprint demonstrated that PMSF had prevented BSA from digestion by Proteinase K, but surprisingly, rExoY was digested (Figure 21B).

Because BSA had been spared when rExoY had not, we examined whether an increased amount of PMSF could prevent rExoY digestion by Proteinase K. The products revealed that at a concentration three times the previous concentration (5.4 mM), we observed complete inhibition of Proteinase K, as rExoY was not digested (Figure 22A). Even though Proteinase K is inhibited by 5.4 mM PMSF, we verified that Proteinase K would not digest rExoY under the conditions of the assay (30°C for 30 min). To simulate the conditions that rExoY would be under in the presence of Proteinase K in the event that basal Proteinase K activity remained, we examined the effect of a one hour incubation at 30°C with 1.8 mM PMSF. The protein profile demonstrated that rExoY was spared (Figure 22B). The two conditions (5.4 mM PMSF and 30°C) were combined to determine how well they would spare rExoY. Based on the protein profile of the reaction products, rExoY was completely spared with the combination of a one hour, 30°C incubation with 5.4 mM PMSF (Figure 22C).

The digested lysate was applied to the ExoY activity assay and assessed for cAMP production with the EIA. rExoY activity was greatly reduced in the presence of the digested lysate (Figure 23).

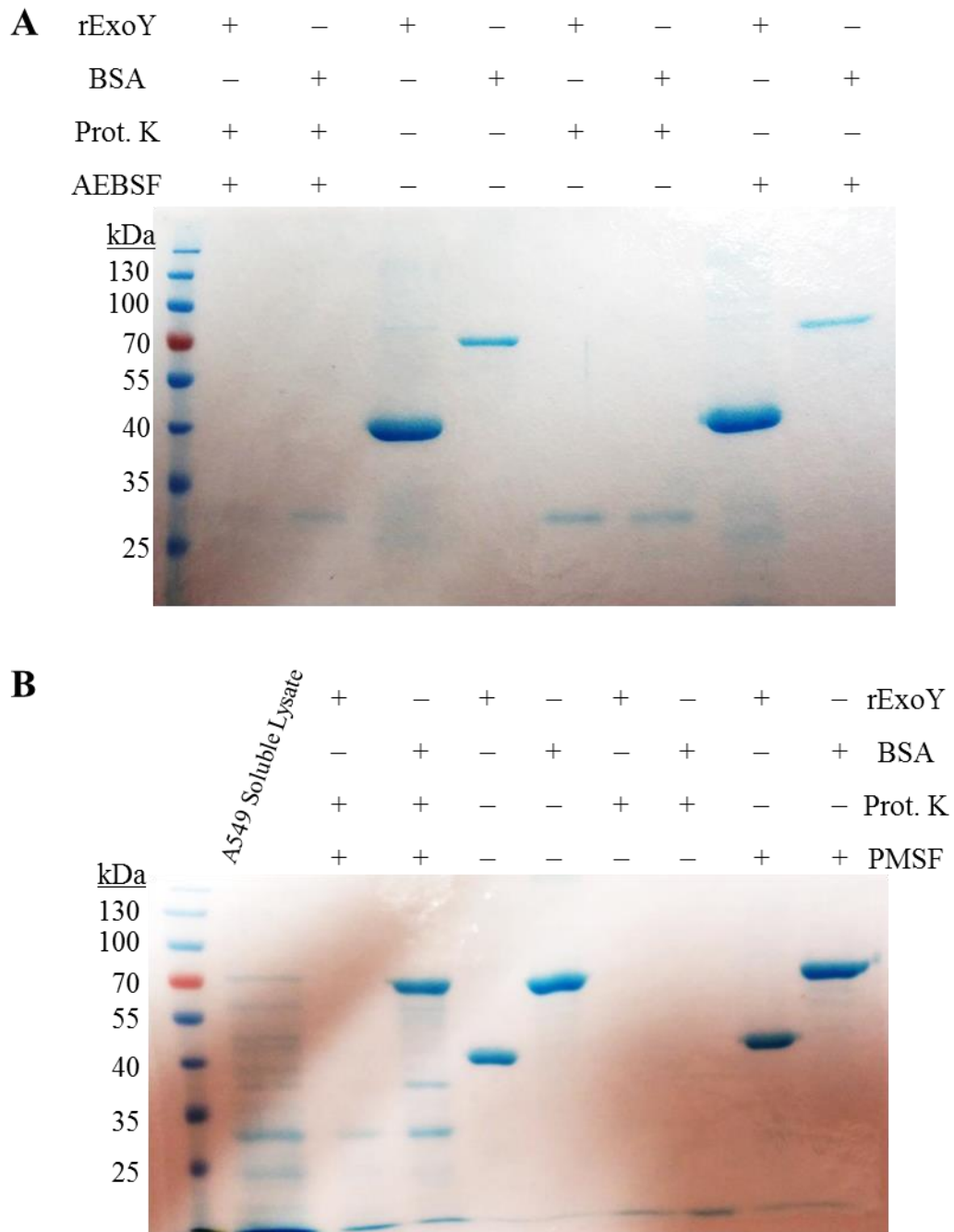


**Figure 21. Effect of Protease Inhibitors on Proteinase K.** **A)** 0.025  $\mu\text{g}/\mu\text{l}$  Proteinase K and 1.6 mM AEBSF were incubated in 20/20 buffer at room temperature for 30 minutes. 6  $\mu\text{g}$  rExoY or BSA (unknown amount) was added and allowed to incubate at 60°C for 1 hour. BSA served as a positive control. **B)** 0.025  $\mu\text{g}/\mu\text{l}$  Proteinase K and 1.8 mM PMSF were incubated in 20/20 buffer at room temperature for 30 minutes. 4  $\mu\text{g}$  rExoY or 4  $\mu\text{g}$  BSA was added and allowed to incubate at 60°C for 1 hour. Protein was analyzed by 10% SDS-PAGE.

rExoY	+	-	+	-	+	-	+	-	-
BSA	-	+	-	+	-	+	-	+	-
Prot. K	+	+	-	-	+	+	-	-	+
PMSF	+	+	-	-	-	-	+	+	+
A549 Lysate	-	-	-	-	-	-	-	-	+

kDa

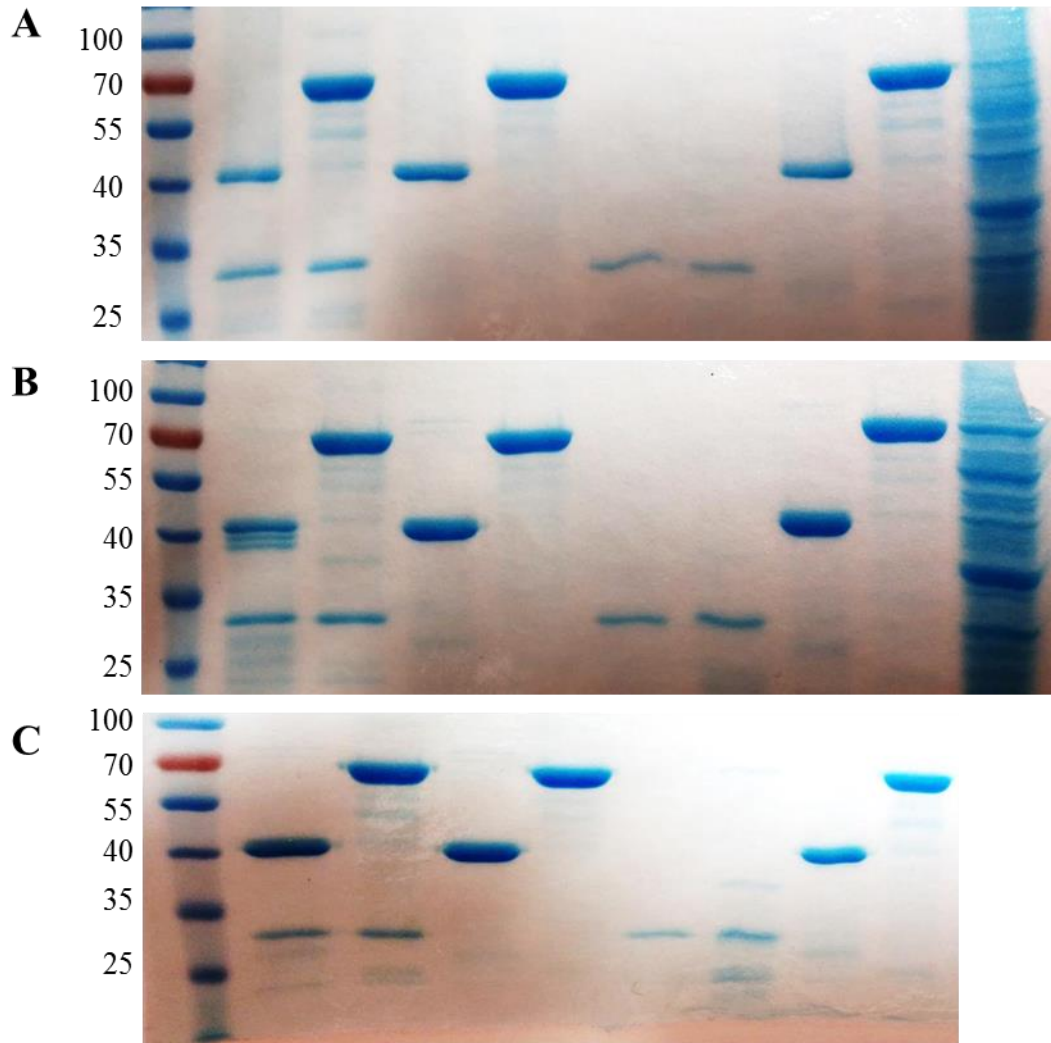


**Figure 22. Effect of Proteinase K and Inhibitor PMSF on rExoY.** **A)** 0.025 µg/µl proteinase K and 1.8 mM PMSF were incubated in 20/20 buffer at room temperature for 30 minutes. 4 µg rExoY or 4 µg BSA was added and allowed to incubate at 30°C for 1 hour. Protein was analyzed by 10% SDS-PAGE. **B)** 0.025 µg/µl Proteinase K and 5.4 mM PMSF were incubated in 20/20 buffer at room temperature for 30 minutes. 4 µg rExoY or 4 µg BSA was incubated at 60°C for 1 hour. **C)** 0.025 µg/µl Proteinase K and 5.4 mM PMSF were incubated in 20/20 buffer at room temperature for 30 minutes. 4 µg rExoY or 4 µg BSA was added and allowed to incubate at 30°C for 1 hour.

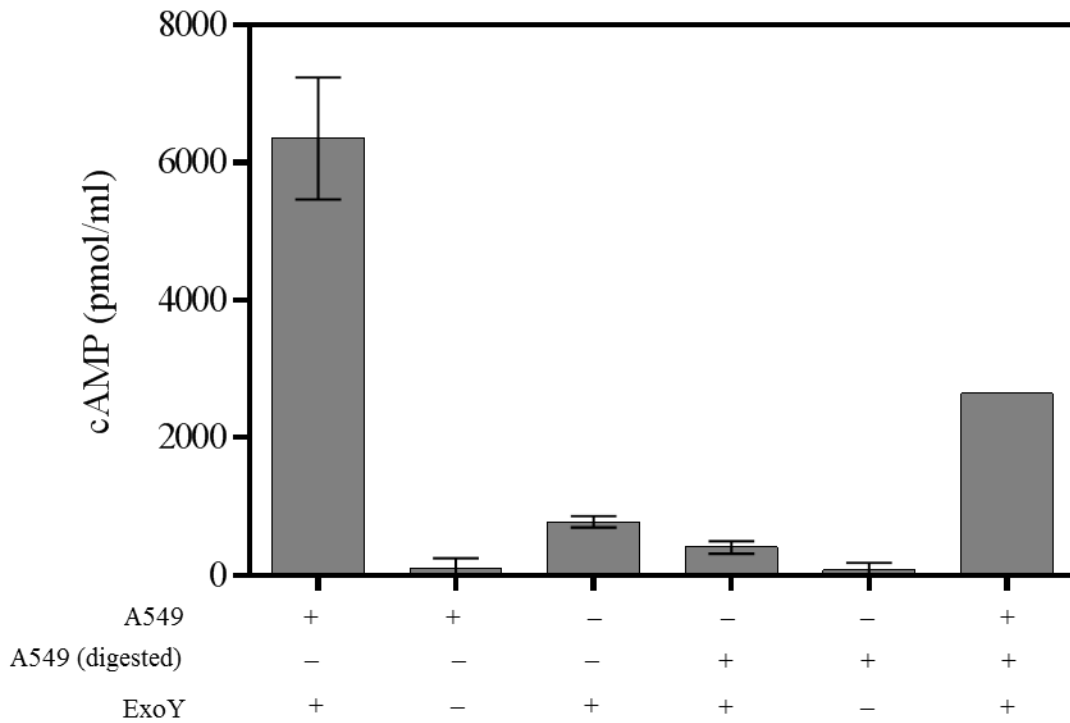


**Figure 23. rExoY Activity after A549 Proteolysis.** The A549 soluble lysate was subjected to digestion by Proteinase K. The digested lysate was assessed for ExoY activity. A reaction with A549 soluble lysate served as a positive control, and reactions without ExoY served as negative controls. A reaction with digested lysate spiked with soluble lysate served as a control to verify the inhibition of Proteinase K. Data represents the arithmetic mean and standard deviation of two independent replicates.

## CHAPTER IV: DISCUSSION

ExoY is a promiscuous nucleotidyl cyclase effector secreted by the T3SS of *Pseudomonas aeruginosa*. The cAMP produced by ExoY promotes hyperphosphorylation of the protein Tau, a microtubule-associated regulatory protein, an effect that impairs microtubule growth [91]. Cellular pathology associated with ExoY includes disruption of the endothelial monolayer, cell rounding, and migration/proliferation impairment; all of which are mediated by cytoskeletal components [89, 90, 92, 104]. The bacterial adenylyl cyclase effectors CyaA and EF are activated by calmodulin, a characteristic not shared with ExoY. The goal of this research was to identify the eukaryotic activator of ExoY.

Early in the project, we intended to use high-performance liquid chromatography (HPLC) to detect the cAMP produced by our reactions. However, technical difficulties and the impracticality of feeding samples into the HPLC at the expense of progress quickly caused us to look for a more efficient method of detection. A cAMP detection kit using radiolabeled cAMP was used by Dr. Benson and provided consistent results in the past [103] – unfortunately, this kit is no longer produced. We elected to use an enzyme immunoassay to detect and quantify rExoY-produced cAMP, and validation of the assay was necessary.

At first, we were concerned that the use of DTT in our activity assay would affect the quantification of cAMP using the Cyclic AMP Direct EIA. We tested the effects of different amounts of DTT on the EIA, and observed that at concentrations at or below 0.2 mM DTT did not affect the assay (Figure 12). The biggest issue we faced in the progress of this project was the variability of the Cyclic AMP Direct EIA; results varied from day

to day and between personnel (Figure 13). Future work should focus on finding a more consistent assay or attempt to standardize the results. We have already started running controls in the assay using known amounts of our own stock of cAMP.

Yahr, *et al.* had determined that heating eukaryotic cell lysate to 100°C for 5 minutes removed the ability to stimulate ExoY and therefore concluded that the activator was proteinaceous in nature [97]. However, we observed a large amount of activity in the A549 cell lysate ultracentrifuge pellet (Figure 17), which could indicate that the activator is a membrane-associated protein or a lipid. Additionally, it could be within a large protein complex, which would be supported by the high level of ExoY specific activity observed in the early SEC fractions (Figure 15). To determine whether the activator is a protein or a lipid, we optimized a Proteinase K digestion reaction to examine whether the activator is indeed a protein.

The control reactions performed as we optimized the Proteinase K digestion demonstrated that AEBSF did not inhibit Proteinase K activity (Figure 21A), despite sources that said otherwise (Gold Biotechnology, n.d.; MP Biomedicals, n.d.). Instead, we turned to another irreversible serine protease inhibitor, PMSF. Our first control reactions used 1.8 mM PMSF – at this concentration, we observed the digestion of rExoY, while BSA was spared (Figure 21B). 1.8 mM PMSF was determined to be an insufficient amount to inhibit all the Proteinase K, and different secondary structures could explain why rExoY was completely digested, while BSA was not; rExoY may have more accessible cut sites for Proteinase K to target. Additionally, the reaction temperature of 60°C could destabilize rExoY, revealing even more cut sites for Proteinase K. Even our typical use of 2 mM DTT could account for this instability – the DTT could prevent

the formation of disulfide bonds that are necessary for stable rExoY structure. The structures of neither native ExoY nor rExoY have been elucidated. Future studies could be focused on learning the structure of ExoY. Circular dichroism spectroscopy is a technique that can be used to reveal the secondary structures of a protein sample; it also would allow us to continue working with rExoY in solution, rather than trying to optimize a crystallization procedure that would account for aggregation and precipitation of rExoY under non-reducing conditions. Additionally, efforts could be made to express ExoY in *P. aeruginosa*, since the instability of rExoY could be due to incorrect folding in the *E. coli* expression strain, BL21.

We were able to identify 5.4 mM PMSF as the optimal concentration to inhibit Proteinase K digestion of rExoY (Figure 22B). Once the Proteinase K digestion reaction was optimized (Figure 22C), we tested the activity level of the soluble lysate after proteolysis, and observed that ExoY activity was completely reduced (Figure 23). Additionally, after the digestion reaction was quenched, we spiked the reaction with soluble lysate; because this reaction still exhibited rExoY activity, Proteinase K had been quenched. Due to reduction in rExoY activity after lysate digestion, we concluded that the activator was proteinaceous.

To verify the results obtained from the Proteinase K digestion, it is recommended that the digestion be repeated. Furthermore, future efforts should be addressed toward a lipolysis or lipid extraction procedure to test rExoY activity in the absence of lipid to verify the Proteinase K digestion data. I would recommend isolating lipid from A549 lysate and purchasing common inner-leaflet phospholipids to examine in the ExoY activity assay.

Now that the activator has been identified as a protein, the biochemical enrichment can be pursued. I would recommend performing an additional size exclusion chromatography step to further separate the activator from the fraction. The fraction with the greatest activity can then be subjected to ion exchange chromatography. However, the salt must be removed from the elutions, as it has been shown that increased salt levels inhibit ExoY activity [103]. Efforts must also be made to optimize the pull-down assay, perhaps using a more specific affinity resin than Ni-NTA HisPur, such as Glutathione-S-Transferase (GST) or a Strep-tag. An immunoprecipitation with  $\alpha$ -rExoY antibody could also prove fruitful.

Work is currently underway to mutagenize each of the five cysteine residues in ExoY in order to understand the role each plays in the structure and function of ExoY. The ultimate goal is to produce an ExoY protein mutant with one or several cysteines that retains its activity but does not require the presence of DTT to remain in solution.

Infection models may also prove insightful into the role that ExoY plays in *P. aeruginosa* virulence. We have lung epithelial and neuronal cell lines at our disposal, but infection of other eukaryotic cells – yeast (*Saccharomyces cerevisiae*), frog (*Xenopus laevis*), plant (*Nicotiana tabacum*), insect (*Drosophila melanogaster*), fish (*Danio rerio*), even nematode (*Caenorhabditis elegans*) or amoeba (*Dictyostelium discoideum*) – could reveal how ExoY assists in pathogenesis in non-human organisms.

Currently ExoY is classified as a class II adenylyl cyclase (a group of bacterial adenylyl cyclases that utilize calmodulin as an activator) despite not being activated by calmodulin [97, 105]. When the identity of the activator is discovered, we can reclassify ExoY into another adenylyl cyclase group.

The activator will ultimately be identified by mass spectroscopy, after which efforts should be made to establish enzyme kinetics and binding data on rExoY and the activator. Given the promiscuous nucleotidyl cyclase activity of ExoY, future work could focus on the mutagenesis of residues in the active site to convert it into a more specific cytidylyl or uridylyl cyclase. In doing so, work could be done to learn about the roles that cyclic cytidine monophosphate (cCMP) or cyclic uridine monophosphate (cUMP) play, not only in a *P. aeruginosa* infection, but in the eukaryotic cell in general.

## **Conclusion**

The role of *Pseudomonas aeruginosa* in nosocomial infections has been well-characterized, particularly as an opportunistic infection of patients who have been mechanically ventilated or those who have cystic fibrosis or burn wounds. Its natural resistance to a wide range of antibiotics, as well as its potent virulence factors, make *P. aeruginosa* a significant risk to public health. Through the identification of the eukaryotic factor that activates ExoY, not only could we more completely understand the role ExoY plays in *P. aeruginosa* virulence, we could justify the reclassification of the bacterial adenylyl cyclase effectors.

## REFERENCES

1. Pseudomonas. LPSN.
2. Bergey's Manual of Determinative Bacteriology.
3. **Caldwell CC, Chen Y, Goetzmann HS, Hao Y, Borchers MT, Hassett DJ, Young LR, Mavrodi D, Thomashow L, Lau GW.** 2009. Pseudomonas aeruginosa exotoxin pyocyanin causes cystic fibrosis airway pathogenesis. *Am. J. Pathol.* **175**:2473–88.
4. **Hugh R, Lessel EF.** 1967. Pseudomonas aeruginosa or Pseudomonas Pyocyanea? *Int. J. Syst. Bacteriol.* **17**:43–51.
5. VetBact.
6. NCBI. Genome.
7. **Church D, Elsayed S, Reid O, Lindsay R, Winston B.** 2006. Burn Wound Infections. *Clin. Microbiol. Rev.* **19**:403.
8. **Koenig SM, Truwit JD.** 2006. Ventilator-associated pneumonia: diagnosis, treatment, and prevention. *Clin. Microbiol. Rev.* **19**:637–57.
9. **Patel PA, Kothari V V, Kothari CR, Faldu PR, Domadia KK, Rawal CM, Bhimani HD, Parmar NR, Nathani NM.** 2014. Draft Genome Sequence of Petroleum Hydrocarbon-Degrading Pseudomonas aeruginosa Strain PK6 , Isolated from the Saurashtra Region of Gujarat , India. *Genome Announc.* **2**:2005–2006.
10. **Chauhan A, Green S, Pathak A, Thomas J.** 2013. Whole-Genome Sequences of Five Oyster-Associated Bacteria Show. *Genome Announc.* **1**:1–2.
11. **Kim W, Tengra FK, Young Z, Shong J, Marchand N, Chan HK, Pangule RC, Parra M, Dordick JS, Plawsky JL, Collins CH.** 2013. Spaceflight promotes biofilm formation by Pseudomonas aeruginosa. *PLoS One* **8**:e62437.
12. **Lessnau K-D, Cunha BA, Dua P, Qarah S.** 2014. Pseudomonas aeruginosa Infections. *MedScape.*
13. **Cole N, Krockenberger M.** 2003. Experimental Pseudomonas aeruginosa keratitis in interleukin-10 gene knockout mice. *Infect. Immun.* **71**:1328–1336.
14. 2014. CDC - Pseudomonas aeruginosa in Healthcare Settings - HAI. CDC.

15. **Rocha LDA Da, Vilela CAP, Cezário RC, Almeida AB, Gontijo Filho P.** 2008. Ventilator-associated pneumonia in an adult clinical-surgical intensive care unit of a Brazilian university hospital: incidence, risk factors, etiology, and antibiotic resistance. *Braz. J. Infect. Dis.* **12**:80–5.
16. **Golia S, K.T. S, C.L. V.** 2013. Microbial profile of early and late onset ventilator associated pneumonia in the intensive care unit of a tertiary care hospital in bangalore, India. *J. Clin. Diagn. Res.* **7**:2462–6.
17. **Goel V, Hogade SA, Karadesai S.** 2012. Ventilator associated pneumonia in a medical intensive care unit: Microbial aetiology, susceptibility patterns of isolated microorganisms and outcome. *Indian J. Anaesth.* **56**:558–62.
18. **Chi SY, Kim TO, Park CW, Yu JY, Lee B, Lee HS, Kim Y Il, Lim SC, Kwon YS.** 2012. Bacterial Pathogens of Ventilator Associated Pneumonia in a Tertiary Referral Hospital. *Tuberc. Respir. Dis. (Seoul).* 32–37.
19. **Taneja N, Chari P, Singh M, Singh G, Biswal M, Sharma M.** 2013. Evolution of bacterial flora in burn wounds: key role of environmental disinfection in control of infection. *Int. J. Burns Trauma* **3**:102–7.
20. **Hsueh P, Teng L, Yang P, Chen Y.** 1998. Persistence of a Multidrug-Resistant *Pseudomonas aeruginosa* Clone in an Intensive Care Burn Unit. *J. Clin. Microbiol.* **36**:1347.
21. **Linsdell P.** 2014. Cystic fibrosis transmembrane conductance regulator chloride channel blockers: Pharmacological, biophysical and physiological relevance. *World J. Biol. Chem.* **5**:26–39.
22. **Buchanan PJ, Ernst RK, Elborn JS, Schock B.** 2009. Role of CFTR, *Pseudomonas aeruginosa* and Toll-like receptors in cystic fibrosis lung inflammation. *Biochem. Soc. Trans.* **37**:863–7.
23. **Hassett DJ.** 1996. Anaerobic production of alginate by *Pseudomonas aeruginosa*: alginate restricts diffusion of oxygen. *J. Bacteriol.* **178**:7322–5.
24. **Coates A.** 1992. Oxygen therapy, exercise, and cystic fibrosis. *CHEST J.* **101**:2–4.
25. **Smith EE, Buckley DG, Wu Z, Saenphimmachak C, Hoffman LR, D'Argenio D a, Miller SI, Ramsey BW, Speert DP, Moskowitz SM, Burns JL, Kaul R, Olson M V.** 2006. Genetic adaptation by *Pseudomonas aeruginosa* to the airways of cystic fibrosis patients. *Proc. Natl. Acad. Sci. U. S. A.* **103**:8487–92.
26. **Poole K.** 2011. *Pseudomonas aeruginosa*: resistance to the max. *Front. Microbiol.* **2**:65.

27. **Rodríguez-Martínez J-M, Poirel L, Nordmann P.** 2009. Molecular epidemiology and mechanisms of carbapenem resistance in *Pseudomonas aeruginosa*. *Antimicrob. Agents Chemother.* **53**:4783–8.
28. **Trias J, Nikaido H.** 1990. Outer Membrane Protein D2 Catalyzes Facilitated Diffusion of Carbapenems and Penems through the Outer Membrane of *Pseudomonas aeruginosa*. *Antimicrob. Agents Chemother.* **34**:52.
29. **Li XZ, Livermore DM, Nikaido H.** 1994. Role of efflux pump(s) in intrinsic resistance of *Pseudomonas aeruginosa*: resistance to tetracycline, chloramphenicol, and norfloxacin. *Antimicrob. Agents Chemother.* **38**:1732–41.
30. **Yates SP, Merrill AR.** 2004. Elucidation of eukaryotic elongation factor-2 contact sites within the catalytic domain of *Pseudomonas aeruginosa* exotoxin A. *Biochem. J.* 563–572.
31. **Wedekind JE, Trame CB, Dorywalska M, Koehl P, Raschke TM, McKee M, FitzGerald D, Collier RJ, McKay DB.** 2001. Refined crystallographic structure of *Pseudomonas aeruginosa* exotoxin A and its implications for the molecular mechanism of toxicity. *J. Mol. Biol.* **314**:823–37.
32. **Jyot J, Balloy V, Jouvion G, Verma A, Touqui L, Huerre M, Chignard M, Ramphal R.** 2011. Type II secretion system of *Pseudomonas aeruginosa*: in vivo evidence of a significant role in death due to lung infection. *J. Infect. Dis.* **203**:1369–77.
33. **Sandkvist M.** 2001. Type II Secretion and Pathogenesis. *Infect. Immun.* **69**:3523–3535.
34. **Farahbakhsh ZT, Baldwin RL, Wisnieskis BJ.** 1986. *Pseudomonas* Exotoxin A: Membrane Binding, Insertion, and Traversal. *J. Biol. Chem.* **261**:11404–11408.
35. **Yates SP, Taylor PL, Jørgensen R, Ferraris D, Zhang J, Andersen GR, Merrill AR.** 2005. Structure–function analysis of water-soluble inhibitors of the catalytic domain of exotoxin A from *Pseudomonas aeruginosa*. *Biochem. J.* 667–675.
36. **Morihara K, Tsuzuki H, Oka T, Inoue H, Ebata M.** 1965. *Pseudomonas aeruginosa* Elastase. *J. Biol. Chem.* **240**:3295–3304.
37. **Bentzmann S De, Polette M.** 2000. *Pseudomonas Aeruginosa* Virulence Factors Delay Airway Epithelial Wound Repair by Altering the Actin Cytoskeleton and Inducing Overactivation of Epithelial Matrix. *Lab. Investig.* **80**:209–219.

38. **Thayer MM, Flaherty KM, McKay DB.** 1991. Three-dimensional structure of the elastase of *Pseudomonas aeruginosa* at 1.5-Å resolution. *J. Biol. Chem.* **266**:2864–71.
39. **Jacquot J, Tournier J, Puchelle E.** 1985. In vitro evidence that human airway lysozyme is cleaved and inactivated by *Pseudomonas aeruginosa* elastase and not by human leukocyte elastase. *Infect. Immun.* **47**:555.
40. **Kuang Z, Hao Y, Walling BE, Jeffries JL, Ohman DE, Lau GW.** 2011. *Pseudomonas aeruginosa* elastase provides an escape from phagocytosis by degrading the pulmonary surfactant protein-A. *PLoS One* **6**:e27091.
41. **Kanthakumar K, Taylor G, Tsang KW, Cundell DR, Rutman A, Smith S, Jeffery PK, Cole PJ, Wilson R.** 1993. Mechanisms of Action of *Pseudomonas aeruginosa* Pyocyanin on Human Ciliary Beat In Vitro. *Infect. Immun.* **61**:2848–2853.
42. **Usher LR, Lawson R a., Geary I, Taylor CJ, Bingle CD, Taylor GW, Whyte MKB.** 2002. Induction of Neutrophil Apoptosis by the *Pseudomonas aeruginosa* Exotoxin Pyocyanin: A Potential Mechanism of Persistent Infection. *J. Immunol.* **168**:1861–1868.
43. **Ran H, Hassett DJ, Lau GW.** 2003. Human targets of *Pseudomonas aeruginosa* pyocyanin. *Proc. Natl. Acad. Sci. U. S. A.* **100**:14315–20.
44. **Hassan HM, Fridovich I.** 1980. Mechanism of the antibiotic action pyocyanine. *J. Bacteriol.* **141**:156–63.
45. **Fyfe J a, Govan JR.** 1980. Alginate synthesis in mucoid *Pseudomonas aeruginosa*: a chromosomal locus involved in control. *J. Gen. Microbiol.* **119**:443–50.
46. **Berry A, DeVault J, Chakrabarty A.** 1989. High osmolarity is a signal for enhanced *algD* transcription in mucoid and nonmucoid *Pseudomonas aeruginosa* strains. *J. Bacteriol.* **171**:2312–2317.
47. **Terry JM, Piña SE, Mattingly SJ.** 1991. Environmental conditions which influence mucoid conversion *Pseudomonas aeruginosa* PAO1. *Infect. Immun.* **59**:471–7.
48. **Pier GB, Coleman F, Grout M, Franklin M.** 2001. Role of Alginate O Acetylation in Resistance of Mucoid *Pseudomonas aeruginosa* to Opsonic Phagocytosis. *Infect. Immun.* **69**:1895–1901.
49. **Terry J, Pina S, Mattingly S.** 1992. Role of energy metabolism in conversion of nonmucoid *Pseudomonas aeruginosa* to the mucoid phenotype. *Infect. Immun.* **60**.

50. **Masi M, Wandersman C.** 2010. Multiple signals direct the assembly and function of a type 1 secretion system. *J. Bacteriol.* **192**:3861–9.
51. **Delepelaire P.** 2004. Type I secretion in gram-negative bacteria. *Biochim. Biophys. Acta* **1694**:149–61.
52. **Dunstan R a, Heinz E, Wijeyewickrema LC, Pike RN, Purcell AW, Evans TJ, Praszquier J, Robins-Browne RM, Strugnell R a, Korotkov K V, Lithgow T.** 2013. Assembly of the type II secretion system such as found in *Vibrio cholerae* depends on the novel Pilotin AspS. *PLoS Pathog.* **9**:e1003117.
53. **Aiello D, Williams JD, Majgier-Baranowska H, Patel I, Peet NP, Huang J, Lory S, Bowlin TL, Moir DT.** 2010. Discovery and characterization of inhibitors of *Pseudomonas aeruginosa* type III secretion. *Antimicrob. Agents Chemother.* **54**:1988–99.
54. **Dewoody RS, Merritt PM, Marketon MM.** 2013. Regulation of the *Yersinia* type III secretion system: traffic control. *Front. Cell. Infect. Microbiol.* **3**:4.
55. **Christie P, Atmakuri K.** 2005. Biogenesis, architecture, and function of bacterial type IV secretion systems. *Annu. Rev. ....*
56. **Christie PJ.** 2004. Type IV secretion: the *Agrobacterium* VirB/D4 and related conjugation systems. *Biochim. Biophys. Acta* **1694**:219–34.
57. **Yen MR, Peabody CR, Partovi SM, Zhai Y, Tseng YH, Saier MH.** 2002. Protein-translocating outer membrane porins of Gram-negative bacteria. *Biochim. Biophys. Acta* **1562**:6–31.
58. **Kostakioti M, Newman C.** 2005. Mechanisms of protein export across the bacterial outer membrane. *J. ...* **187**:4306–4314.
59. **Pukatzki S, Ma AT, Sturtevant D, Krastins B, Sarracino D, Nelson WC, Heidelberg JF, Mekalanos JJ.** 2006. Identification of a conserved bacterial protein secretion system in *Vibrio cholerae* using the *Dictyostelium* host model system. *Proc. Natl. Acad. Sci. U. S. A.* **103**:1528–33.
60. **Mougous J, Cuff M, Raunser S, Shen A.** 2006. A virulence locus of *Pseudomonas aeruginosa* encodes a protein secretion apparatus. *Science (80-. )*. **312**:1526–1530.
61. **Cascales E.** 2008. The type VI secretion toolkit. *EMBO Rep.* **9**:735–41.
62. **Filloux A.** 2009. The type VI secretion system: a tubular story. *EMBO J.* **28**:309–10.

63. **Filloux A.** 2013. The rise of the Type VI secretion system. *F1000Prime Rep.* **5**:52.
64. **Zheng Z, Chen G, Joshi S, Brutinel ED, Yahr TL, Chen L.** 2007. Biochemical characterization of a regulatory cascade controlling transcription of the *Pseudomonas aeruginosa* type III secretion system. *J. Biol. Chem.* **282**:6136–42.
65. **Dasgupta N, Ashare A, Hunninghake GW, Yahr TL.** 2006. Transcriptional induction of the *Pseudomonas aeruginosa* type III secretion system by low Ca<sup>2+</sup> and host cell contact proceeds through two distinct signaling pathways. *Infect. Immun.* **74**:3334–41.
66. **Halavaty AS, Borek D, Tyson GH, Veessenmeyer JL, Shuvalova L, Minasov G, Otwinowski Z, Hauser AR, Anderson WF.** 2012. Structure of the type III secretion effector protein ExoU in complex with its chaperone SpcU. *PLoS One* **7**:e49388.
67. **Sato H, Frank DW.** 2004. ExoU is a potent intracellular phospholipase. *Mol. Microbiol.* **53**:1279–90.
68. **Halavaty AS, Borek D, Tyson GH, Veessenmeyer JL, Shuvalova L, Minasov G, Otwinowski Z, Hauser AR, Anderson WF.** 2012. Structure of the type III secretion effector protein ExoU in complex with its chaperone SpcU. *PLoS One* **7**:e49388.
69. **Anderson DM, Schmalzer KM, Sato H, Casey M, Terhune SS, Haas AL, Feix JB, Frank DW.** 2011. Ubiquitin and ubiquitin-modified proteins activate the *Pseudomonas aeruginosa* T3SS cytotoxin, ExoU. *Mol. Microbiol.* **82**:1454–67.
70. **Goehring U, Schmidt G, Pederson KJ, Aktories K, Barbieri JT.** 1999. The N-terminal Domain of *Pseudomonas aeruginosa* Exoenzyme S Is a GTPase-activating Protein for Rho GTPases. *J. Biol. Chem.* **274**:36369–36372.
71. **Iglewski BH, Sadoff J, Bjorn MJ, Maxwell ES.** 1978. *Pseudomonas aeruginosa* exoenzyme S: an adenosine diphosphate ribosyltransferase distinct from toxin A. *Proc. Natl. Acad. Sci. U. S. A.* **75**:3211–5.
72. **Ganesan a K, Vincent TS, Olson JC, Barbieri JT.** 1999. *Pseudomonas aeruginosa* exoenzyme S disrupts Ras-mediated signal transduction by inhibiting guanine nucleotide exchange factor-catalyzed nucleotide exchange. *J. Biol. Chem.* **274**:21823–9.
73. **Lee VT, Smith RS, Tümmler B, Lory S.** 2005. Activities of *Pseudomonas aeruginosa* effectors secreted by the Type III secretion system in vitro and during infection. *Infect. Immun.* **73**:1695–705.

74. **Shaver CM, Hauser AR.** 2004. Relative Contributions of *Pseudomonas aeruginosa* ExoU, ExoS, and ExoT to Virulence in the Lung. *Infect. Immun.* **72**:6969.
75. **Wolfgang MC, Kulasekara BR, Liang X, Boyd D, Wu K, Yang Q, Miyada CG, Lory S.** 2003. Conservation of genome content and virulence determinants among clinical and environmental isolates of *Pseudomonas aeruginosa*. *Proc. Natl. Acad. Sci. U. S. A.* **100**:8484–9.
76. **Fu H, Coburn J, Collier RJ.** 1993. The eukaryotic host factor that activates exoenzyme S of *Pseudomonas aeruginosa* is a member of the 14-3-3 protein family. *Proc. Natl. Acad. Sci. U. S. A.* **90**:2320–4.
77. **Van Heusden GPH.** 2005. 14-3-3 Proteins: Regulators of Numerous Eukaryotic Proteins. *IUBMB Life* **57**:623–9.
78. **Krall R, Schmidt G, Aktories K, Barbieri T.** 2000. *Pseudomonas aeruginosa* ExoT Is a Rho GTPase-Activating Protein. *Infect. Immun.* **68**:6066–6068.
79. **Sun J, Barbieri JT.** 2003. *Pseudomonas aeruginosa* ExoT ADP-ribosylates CT10 regulator of kinase (Crk) proteins. *J. Biol. Chem.* **278**:32794–800.
80. **Yahr T, Barbieri J, Frank D.** 1996. Genetic relationship between the 53-and 49-kilodalton forms of exoenzyme S from *Pseudomonas aeruginosa*. *J. Bacteriol.* **178**.
81. **Vance RE, Rietsch A, Mekalanos JJ.** 2005. Role of the type III secreted exoenzymes S, T, and Y in systemic spread of *Pseudomonas aeruginosa* PAO1 in vivo. *Infect. Immun.* **73**:1706–13.
82. **Sutherland E.** 1992. Studies on the Mechanism of Hormone Action, p. . *In* Lindsten, J (ed.), *Nobel Lectures, Physiology or Medicine 1971-1980*. World Scientific Publishing Co., Singapore.
83. **Walsh D, Patten S Van.** 1994. Multiple pathway signal transduction by the cAMP-dependent protein kinase. *FASEB J.* 1227–1236.
84. **Soderling TR.** 1975. Regulation of glycogen synthetase. Specificity and stoichiometry of phosphorylation of the skeletal muscle enzyme by cyclic 3': 5'-AMP-dependent protein kinase. *J. Biol. Chem.* **250**:5407–5412.
85. **Smith SB, White HD, Siegel JB, Krebs EG.** 1981. Cyclic AMP-dependent protein kinase I: cyclic nucleotide binding, structural changes, and release of the catalytic subunits. *Proc. Natl. Acad. Sci. U. S. A.* **78**:1591–5.
86. **Seifert R, Hartwig C, Wolter S, Reinecke D, Burhenne H, Kaefer V, Munder A, Tummler B, Schwede F, Grundmann M, Kostenis E, Frank DW, Beckert**

- U. 2013. *Pseudomonas aeruginosa* ExoY, a cyclic GMP- and cyclic UMP-generating nucleotidyl cyclase. *BMC Pharmacol. Toxicol.* **14**:O36.
87. **Pietrobon M, Zamparo I, Maritan M, Franchi SA, Pozzan T, Lodovichi C.** 2011. Interplay among cGMP, cAMP, and Ca<sup>2+</sup> in living olfactory sensory neurons in vitro and in vivo. *J. Neurosci.* **31**:8395–405.
88. **Brown R, Strassmaier T.** 2005. The pharmacology of cyclic nucleotide-gated channels: emerging from the darkness. *Curr. Pharm. ...* **12**:3597–3613.
89. **Vallis AJ, Finck-Barbancon V, Yahr TL, Frank DW.** 1999. Biological Effects of *Pseudomonas aeruginosa* Type III-Secreted Proteins on CHO Cells. *Infect. Immun.* **67**:2040–2044.
90. **Sayner SL, Frank DW, King J, Chen H, VandeWaa J, Stevens T.** 2004. Paradoxical cAMP-induced lung endothelial hyperpermeability revealed by *Pseudomonas aeruginosa* ExoY. *Circ. Res.* **95**:196–203.
91. **Ochoa CD, Alexeyev M, Pastukh V, Balczon R, Stevens T.** 2012. *Pseudomonas aeruginosa* exotoxin Y is a promiscuous cyclase that increases endothelial tau phosphorylation and permeability. *J. Biol. Chem.* **287**:25407–18.
92. **Stevens TC, Ochoa CD, Morrow KA, Robson MJ, Prasain N, Zhou C, Alvarez DF, Frank DW, Balczon R, Stevens T.** 2014. The *Pseudomonas aeruginosa* exoenzyme Y impairs endothelial cell proliferation and vascular repair following lung injury. *Am. J. Physiol. Lung Cell. Mol. Physiol.*
93. **Tanaka T.** 1988. Calmodulin-dependent calcium signal transduction. *Jpn. J. Pharmacol.* **46**:101–107.
94. **Guo Q, Shen Y, Lee Y-S, Gibbs CS, Mrksich M, Tang W-J.** 2005. Structural basis for the interaction of *Bordetella pertussis* adenylyl cyclase toxin with calmodulin. *EMBO J.* **24**:3190–201.
95. **Guo Q, Jureller JE, Warren JT, Solomaha E, Florián J, Tang W-J.** 2008. Protein-protein docking and analysis reveal that two homologous bacterial adenylyl cyclase toxins interact with calmodulin differently. *J. Biol. Chem.* **283**:23836–45.
96. **Ulmer TS, Soelaiman S, Li S, Klee CB, Tang W-J, Bax A.** 2003. Calcium dependence of the interaction between calmodulin and anthrax edema factor. *J. Biol. Chem.* **278**:29261–6.
97. **Yahr TL, Vallis AJ, Hancock MK, Barbieri JT, Frank DW.** 1998. ExoY, an adenylate cyclase secreted by the *Pseudomonas aeruginosa* type III system. *Proc. Natl. Acad. Sci. U. S. A.* **95**:13899–904.

98. **Hritonenko V, Mun JJ, Tam C, Simon NC, Barbieri JT, Evans DJ, Fleiszig SMJ.** 2011. Adenylate cyclase activity of *Pseudomonas aeruginosa* ExoY can mediate bleb-niche formation in epithelial cells and contributes to virulence. *Microb. Pathog.* **51**:305–12.
99. **Ladant D, Brezins C, Alonsos J, Crenons I, Guiso N.** 1986. Bordetella pertussis Adenylate Cyclase. *J. Biol. Chem.* **261**:16264–16269.
100. **Ladant D.** 1988. Interaction of Bordetella pertussis Adenylate Cyclase with Calmodulin. *J. Biol. Chem.* **263**:2612–2618.
101. **Leppla SH.** 1982. Anthrax toxin edema factor : A bacterial adenylate cyclase that increases cyclic AMP concentrations in eukaryotic cells *Biochemistry* : Leppla **79**:3162–3166.
102. **Galindo S.** No Title.
103. **Benson M.** 2009. Understanding the Mechanisms Mediating the Activation of the *Pseudomonas aeruginosa* Toxins ExoU and ExoY by their Cognate Activators. Medical College of Wisconsin.
104. **Soong G, Parker D, Magargee M, Prince AS.** 2008. The type III toxins of *Pseudomonas aeruginosa* disrupt epithelial barrier function. *J. Bacteriol.* **190**:2814–21.
105. **Danchin A.** 1993. Phylogeny of adenylyl cyclases. *Adv. Second Messenger Phosphoprotein Res.* **27**:109–162.